

Mariano Kappes*, Mariano Iannuzzi, Raúl B. Rebak and Ricardo M. Carranza

Sulfide stress cracking of nickel-containing low-alloy steels

Abstract: Low-alloy steels (LAS) are extensively used in oil and gas (O&G) production due to their good mechanical properties and low cost. Even though nickel improves mechanical properties and hardenability with low penalty on weldability, which is critical for large subsea components, nickel content cannot exceed 1-wt% when used in sour service applications. The ISO 15156-2 standard limits the nickel content in LAS on the assumption that nickel concentrations above 1-wt% negatively impact sulfide stress cracking (SSC) resistance. This restriction excludes a significant number of high-strength and high-toughness alloys, such as Ni-Cr-Mo (e.g., UNS G43200 and G43400), Ni-Mo (e.g., UNS G46200), and Ni-Cr-Mo-V grades, from sour service applications and can be used only if successfully qualified. However, the standard is based on controversial research conducted more than 40 years ago. Since then, researchers have suggested that it is the microstructure that determines SSC resistance, regardless of Ni content. This review summarizes the advantages and disadvantages of nickel-containing LAS in terms of strength, weldability, hardenability, potential weight savings, and cost reduction. Likewise, the state of knowledge on the effect of nickel on hydrogen absorption as well as SSC initiation and propagation kinetics is critically reviewed.

Keywords: embrittlement; hydrogen nickel; low-alloy steel; microstructure; sulfide stress cracking.

DOI 10.1515/correv-2014-0027

Received June 19, 2014; accepted August 8, 2014; previously published online September 18, 2014

*Corresponding author: **Mariano Kappes**, Comisión Nacional de Energía Atómica, Instituto Sabato (UNSAM/CNEA), Av. Gral. Paz 1499, San Martín, Buenos Aires 1650, Argentina, e-mail: marianokappes@gmail.com

Mariano Iannuzzi: General Electric, Oil and Gas, Eyvind Lyches vei 10, Sandvika, Bærum NO1338, Norway

Raúl B. Rebak: General Electric, Global Research Center, 1 Research Circle, Schenectady, NY 12309, USA

Ricardo M. Carranza: Comisión Nacional de Energía Atómica, Instituto Sabato (UNSAM/CNEA), Av. Gral. Paz 1499, San Martín, Buenos Aires 1650, Argentina

1 Introduction

Low-alloy steels (LASs) are extensively used in oil and gas (O&G) production because of their good mechanical properties and low cost. Use of these materials in environments containing H_2S is governed by the ISO 15156-2 standard (NACE-ISO, 2001), “Petroleum and natural gas industries – materials for use in H_2S -containing environments in oil and gas production”. LAS with additions of molybdenum, chromium, and Ni combine high strength with adequate toughness. When subjected to the correct combination of heat treatments, LAS with Ni, Mo, and Cr contents in the 1.00-, 0.25-, and 1.00-wt% range, respectively, exhibit either fully tempered martensitic or bainitic structures through-thickness.

Typical Cr-Ni-Mo LAS have yield strength (YS) values above 415–560 MPa (60–80 ksi) and minimum tangential Charpy V-notch (CVN) impact energy values above 42 J at $-60^\circ C$ (DNV, 2012; ISO, 2009). Carbon equivalent (CE), which empirically quantifies the effect of the main alloying elements on weldability relative to carbon, is normally above 0.42, and it is only limited to assure proper weldability. ISO 15156-2 limits the hardness of the base metal to a maximum of 250 HV (22 HRC) (and 275 HV for weld caps) to assure adequate sour service performance. Despite the beneficial effects of nickel in terms of mechanical, metallurgical, and technological properties Ni content cannot exceed 1-wt% in sour service O&G production environments due to sulfide stress cracking (SSC) concerns.

As previously reviewed by Craig (1982, 1988), steels with YS higher than 1035 MPa (150 ksi) are susceptible to hydrogen embrittlement (HE) independently of their composition. ISO 15156-2 (NACE-ISO, 2001) 22 HRC limit roughly corresponds to an ultimate tensile strength (UTS) of 800 MPa (116 ksi) (Boyer, 1976). In terms of YS, Cr-Mo tubulars with specified minimum yield strength (SMYS) of 760 MPa (110 ksi) are generally accepted for sour service within ISO 15156-2 limitations (NACE-ISO, 2001). The remainder of this review focuses on alloys within ISO 15156-2 strength and hardness boundaries.

This review is divided into three main sections. First, the potential commercial impact of high-strength and high-toughness nickel alloy steels is presented. Second, the effect of nickel on the physical metallurgy of LAS is discussed, and finally, the role of nickel on SSC performance is critically reviewed.

2 Potential market of Ni-containing LAS for sour service applications

In the past two decades, the O&G industry has witnessed a shift in operating conditions driven by the need to (i) develop high pressure, i.e., 103 MPa, high temperature, i.e., 177°C (HPHT), and extreme high pressure, i.e., 206 MPa, extreme high temperature, i.e., 250°C, (xHPHT) fields (API, 2013) with a high potential for reservoir souring, and (ii) operate in extremely low-temperature conditions (API, 2013; Hope, 2008; Paterson, 2012; Schillmoller & Craig, 1987). As the development of such reservoirs becomes economically feasible due to the steady increase in crude oil prices, the O&G industry could potentially face a technological roadblock given the limitations mandated by international materials standards.

It is believed that in the 10- to 15-year horizon, materials for the so-called pressure envelope will have to meet at least one of these three key requirements:

1. Homogeneous through-thickness YS levels above 690 MPa (100 ksi) (Borik, Anselme, deSivry, Bousset, & Bonnet, 1982; Krog & Qvale, 2012; Paterson, 2012)
2. Ductile-to-brittle transition temperatures (DBTTs) below -60°C (Horn, 2012; Horn & Hauge, 2011; ISO, 2010a; Kharionovskii, 1983)
3. Adequate sour service resistance (Hamby, 1975; Shaughnessy, Romo, & Soza, 2003).

These requirements will equally affect forgings, castings, and oil country tubular goods (OCTGs) but will be critical for thick-wall components where homogeneous through-thickness properties are difficult to achieve (Krog & Qvale, 2012; Welsch, Bruch, & Østby, 2011). As will be explained herein, nickel additions to LAS improve hardenability and lower the DBTT with limited effect on CE. No other alloying element improves strength and toughness simultaneously without a significant penalty on weldability. Increase in through-thickness strength can lead to potential weight savings, which directly translates to cost savings.

Today, the most common applications of nickel-containing LAS in H₂S-free environments are valves, pumps, piping and vessels processing and handling liquefied

petroleum gas, where service temperatures can be below -100°C (Farrar, 2004). In H₂S-containing environments, potential applications of nickel alloy steels include hubs, spools, large valve bodies and bonnets, pup pieces, connectors, couplers, risers, turbine stems/shafts, and OCTGs. Nickel additions to LAS are advantageous for components designed to sustain high system pressures and/or equipment that may experience rapid decompression and severe cooling caused by adiabatic expansion (i.e., Joule-Thomson effect). In addition, nickel alloy steels are essential for the development of O&G fields in the arctic region (Cheng & Ou, 1978; Heidersbach, 2010; Horn, Østby, Hauge, & Aubert, 2012; Krog & Qvale, 2012). As stated by Farrar (2004), nickel steels in the 1.5- to 3.5-wt% range can also be used in the manufacture of fatigue-loaded and rotating engineering components such as shafts and rotors, as they offer enhanced fatigue performance when compared with conventional C-Mn steels.

ISO restriction excludes a significant number of high-strength and high-toughness alloys, such as Ni-Cr-Mo (e.g., UNS G43200 and G43400), Ni-Mo (e.g., UNS G46200), and Ni-Cr-Mo-V grades, from sour service applications and must be qualified for use in H₂S-containing environments. Previous efforts to lift the 1-wt% Ni maximum restriction were unsuccessful due to differences in the interpretation of the existing results at the time of the NACE MR0175 committee votes (B. Craig, personal communication, 2014). It is also interesting to remark that NACE standard MR 0103, “Materials resistant to sulfide stress cracking in corrosive petroleum refining environments” (ANSI-NACE, 2012), which was adapted from ISO 15156 to cover sour petroleum refining and related processing environments containing H₂S, does not impose any restriction in terms of nickel content.

Elucidating the role of nickel on SSC resistance is of great technological and scientific relevance. Qualifying high-strength and high-toughness LAS with nickel contents above the current 1-wt% limit for sour service will be a technology enabler for the development of the O&G reservoirs of the future.

3 Effect of nickel on microstructure, processing, and mechanical properties of LAS

Observation of the Fe-Ni phase diagram reveals that nickel remains in solid solution in the ferrite phase up to about 7-wt% (Craig, 1982), providing an additional increment in strength that is independent of tempering temperature (Craig, Brownlee, & Bruno, 1990; Grange, 1973). Nickel

influences phase transformation kinetics as well as segregation. Therefore, it has a strong effect on mechanical and technological properties. This section reviews the effects of nickel on austenite and martensite transformation reactions, segregation of metalloid elements, hardenability, fracture toughness, and weldability.

3.1 Effects of Ni on austenite and martensite transformation

Nickel, an austenite-stabilizing element, decreases A_{c_1} and A_{c_3} (Andrews, 1965), i.e., the lower and upper austenite transformation temperatures, respectively, impacting optimal austenitizing and tempering temperatures. Researchers have proposed different empirical formulas to relate A_{c_1} and A_{c_3} with alloy composition. The two most frequently used equations are shown below, which are valid for LASs with $C < 0.6\text{-wt}\%$, $Cr < 5\text{-wt}\%$, $Ni < 5\text{-wt}\%$, $W < 4.1\text{-wt}\%$, and $Mo < 5.4\text{-wt}\%$ (Andrews, 1965),

$$A_{c_1} = 723 - 10.7 \cdot Mn - 16.9 \cdot Ni + 29.1 \cdot Si + 16.9 \cdot Cr + 290 \cdot As + 6.38 \cdot W \quad (1)$$

$$A_{c_3} = 910 - 203 \cdot \sqrt{C} - 15.2 \cdot Ni + 44.7 \cdot Si + 104 \cdot V + 31.5 \cdot Mo + 13.1 \cdot W, \quad (2)$$

where A_{c_1} and A_{c_3} are given in °C and all compositions are in wt%.

The A_{c_1} of a C-Mn steel (i.e., 1.0-wt% Mn and maximum 0.15-wt% Si) decreases approximately 85°C (i.e., from 708°C down to 623°C) when Ni content is increased to 5-wt%. Given that Ni is often combined with Cr and Mo, the effect on A_{c_1} can be even more pronounced. As a result, tempering temperatures, which can be as high as 650°C for standard 1Ni 0.25Cr LAS, have to be modified accordingly to prevent austenite transformation. Austenite that forms as a consequence of an improper heat treatment can lead to untempered martensite upon cooling or due to plastic stress or strain, as explained below, greatly affecting sour service performance.

Nickel also decreases the martensite start temperature, M_s , i.e. the temperature at which martensite starts to form upon rapid cooling. The following empirical equation was presented by Andrews (1965) and is valid for the same composition range as Equations 1 and 2:

$$M_s = 539 - 423 \cdot C - 30.4 \cdot Mn - 17.7 \cdot Cr - 7.5 \cdot Mo \quad (3)$$

M_s determines the type of martensite, i.e., lath or plate, that forms upon cooling. Lath martensite has an array of tangled dislocations inside the crystals and becomes

predominant when $M_s > 315^\circ\text{C}$, whereas plate martensite is internally twinned and dominates at $M_s < 205^\circ\text{C}$ (Krauss, 1989). A mixture of both types of martensite is obtained at an intermediate temperature range (Krauss, 1989). Equation 3 shows that carbon has the largest effect on M_s temperature, followed by Mn, Ni, and Cr. For low- and medium-carbon steels as well as LAS, microstructure consists mainly of lath martensite.

Low M_s temperatures can lead to retained austenite at room temperature. The main risk of retained austenite is that it could transform to untempered martensite with stress or strain application, impacting negatively on SSC resistance (Snape, 1968b). In this regard, strain-induced martensite transformation could readily occur during cold forming and machining operations conducted post-heat treatment.

Retained austenite in interlath martensite can also transform to cementite, giving interlath carbides or untempered martensite, both of which can negatively affect fracture toughness (Craig, 1982; Williamson, Schupmann, Materkowski, & Krauss, 1979). The volume of retained austenite, V_γ , depends on the value of M_s and the minimum temperature value reached during quenching, T_q (Koistinen & Marburger, 1959),

$$V_\gamma = e^{[0.011(M_s - T_q)]} \quad (4)$$

According to Equation 4, a non-zero percentage of retained austenite is present at any temperature, suggesting that there is always some finite amount of retained austenite in the final microstructure.

A martensite finish temperature, M_f , can be defined as the temperature at which the amount of martensite is 99%. Equations 3 and 4 can be combined into an expression that relates the increment in retained austenite after a given Ni addition:

$$\frac{V_\gamma^{\text{base alloy} + \text{Ni}}}{V_\gamma^{\text{base alloy}}} = e^{[0.1947 \cdot \text{Ni}]} \quad (5)$$

This equation indicates that a 1-wt% Ni addition to a Ni-free base alloy would result in an increase in retained austenite of 21%, a 2% addition, in an increase of 48%.

Procedures to reduce the amount of retained austenite include (i) a cryogenic treatment and (ii) conditioning of the retained austenite (Prabhudev, 1988), which find wider application in higher-alloyed tool steels, where the amount of retained austenite is considerably larger than on LAS. The cryogenic treatment involves immersion of the as-quenched steel in liquid nitrogen to obtain sub-zero temperatures that favor retained austenite transformation

to martensite (Zhirafar, Rezaeian, & Pugh, 2007). Conditioning of retained austenite is a dual tempering and cooling treatment. A first temper in the 450°C–600°C range favors the precipitation of carbides in austenite. As a result, the amount of elements in solid solution decreases and M_s increases. Tempering therefore conditions the austenite, which transforms to martensite upon cooling. Finally, a second temper is required to temper the fresh martensite.

Retained austenite in LAS can also transform to carbides in the 200°C–400°C range (Sarıkaya, Jhingan, & Thomas, 1983; Williamson et al., 1979). This reaction can lead to tempered martensite embrittlement due to transformation of retained austenite into interlath M_3C films (Sarıkaya et al., 1983). This form of embrittlement yields a transgranular fracture with respect to prior austenite grains (Sarıkaya et al., 1983). However, for sour service applications tempering is conducted at higher temperatures, i.e., typically above 610°C (DNV, 2012; NACE-ISO, 2001; Payer, Pednekar, & Boyd, 1986), reducing the risk of this form of embrittlement.

3.2 Segregation of metalloid elements

Ni and Cr, especially when present together, can promote segregation of metalloid elements such as antimony, phosphorus, tin, and arsenic to prior austenite grain boundaries (Mulford, McMahon, Pope, & Feng, 1976a). This process is believed to be the root cause of temper embrittlement (Davis, 1990). Depth profiling with Ar^+ sputtering of samples fractured inside the Auger electron spectroscopy vacuum chamber revealed that segregated phosphorus was confined within two atomic layers of the grain boundary, whereas Ni segregation was five times wider (Mulford, McMahon, Pope, & Feng, 1976b; Viswanathan, 1971). Segregation is promoted by slowly cooling through the 350°C–600°C range, by tempering, or by service in this region (Craig, 1982; Mulford et al., 1976b). Although temper embrittlement concerns impose an upper limit to the maximum allowable operating temperature, segregation occurs at temperatures significantly higher than the reported high temperature values (i.e., 250°C) of the xHPHT fields (API, 2013).

The main consequence of temper embrittlement is a decrease in toughness characterized by an increase in the DBTT to values that can exceed room temperature (Viswanathan, 1971). The increment in DBTT temperature is controlled by three factors, namely, the concentration of impurities at grain boundary, the hardness level, and the prior austenite grain size (Mulford et al., 1976b). For a

given austenite grain size and impurity level, harder steels experience a more pronounced shift in DBTT.

Tempering at temperatures in the 350°C–600°C range minimize temper embrittlement or can reverse the process altogether (Viswanathan, 1971) if sufficient time (i.e., the exposure time depends on the dimensions of the component, but it is typically one hour for laboratory-sized specimens) is given to dissolve segregated elements back into the grains. Rapid cooling through the temper embrittlement range prevents segregation during cooling; but this is unfeasible in heavy-wall equipment. Other solutions include a decrease in metalloid concentration and molybdenum additions. Phosphorus (P) contents as low as 0.02-wt% can increase the DBTT of Mo-free Ni-Cr LAS heat treated at 500°C (McMahon, Cianelli, & Feng, 1977) by as much as 60°C. As a reference, P content in UNS 43400 and other nickel alloy steels is limited to a maximum of 0.035-wt%, so resistance to temper embrittlement is imparted by adding scavengers and/or imposing stricter P composition limits (ASTM, 2010a; VGS, 2012a, b, d). In this regard, molybdenum acts as a P scavenger, as long as it is in solid solution rather than in carbides (McMahon et al., 1977). Lowalloy UNS G43400 Cr-Ni-Mo steel, which has around 0.25-wt% of Mo, is immune to temper embrittlement (Philip & McCaffrey, 1990).

A synergy between temper embrittlement and hydrogen-assisted cracking has been reported by Craig and Krauss (1980). In the presence of hydrogen, P segregation can contribute to intergranular HE of Ni-Cr-Mo steels that are *a priori* immune to temper embrittlement. This form of embrittlement was observed when steels such as UNS G43400 and UNS G41400 were quenched and tempered to a strength level in excess of 1000 MPa (145 ksi) (Craig & Krauss, 1980; Oriani, 1987), i.e., at temperatures below 500°C, and it was associated with a phosphorus-hydrogen interaction (Craig & Krauss, 1980). This type of failure can be prevented by rapid quenching and tempering at temperatures above 500°C.

3.3 Effects of Ni on hardenability

For heavy section, hardenability is perhaps the most critical functional property of the steel. As explained by Krauss (2005a), the term “hardenability” relates to the suppression of diffusion-controlled transformations and to the propensity of a steel to harden under various cooling conditions. As a result, hardenability can be considered a property of the material that measures the capacity of a steel to transform partially or completely from austenite to some percentage of martensite at a given depth upon

cooling (Siebert, Doane, & Breen, 1977). Hardenability is therefore a function of steel composition and microstructure exclusively.

The hardenability of steel is traditionally determined by measuring the hardness depth profile distribution of a sample as a function of different heat treatment parameters. Quantitative measures of hardenability include Grossmann and Bain ideal size/diameter approach and the use of Jominy curves (Kirkaldy & Feldman, 1989; Kuch, 1990). The ideal diameter of a steel is defined as the diameter of a bar that, when quenched by a theoretically ideal quench, will have 50% martensite in its center. The ideal size is thus a true measure of the hardenability associated with a given steel composition. An ideal quench has the ability to lower the temperature of the steel surface instantaneously to the temperature of the bath and keep it there indefinitely (Krauss, 2005a). Quenching in iced and violently circulated brine closely approaches ideal quench conditions. The Jominy and Boegehold test method, standardized as ASTM A255 and SAE J406, characterizes hardenability of a steel using a single specimen rather than from a series of round bars. The hardenability of the steel is then determined by measuring the depth of the inflexion point in a “hardness vs. distance from quench end” diagram.

Researchers have proposed different models to correlate ideal diameter with degree of alloying. If the ideal diameter of a plain carbon steel (D_{IC}) with a given carbon content and austenite grain size is known, the ideal diameter of a LAS (D_I) of similar composition is obtained by multiplying D_{IC} by the multiplying factor of each alloying element (DeRetana & Doane, 1971),

$$D_I = D_{IC} \cdot f_{Mn} \cdot f_{Cr} \cdot f_{Mo} \cdot f_{Ni} \cdot f_V \cdot f_{Si} \cdot \dots \quad (6)$$

In general, the multiplying factor of a given alloying element increases with concentration (Figure 1). Multiplying factors are not constant and change appreciably when comparing different steels families, e.g., medium-carbon LASs and carburizing steels (DeRetana & Doane, 1971; Grange, 1973; Krauss, 2005a; Scoonover & Arnson, 1984). In general, the multiplying factor for nickel is smaller than the one for the rest of the common alloying elements, like Mn, Cr, Si, and Mo (DeRetana & Doane, 1971; Grange, 1973; Krauss, 2005a; Scoonover & Arnson, 1984), suggesting a less pronounced effect on hardenability. However, as shown by Grange (1973), nickel has a marked effect on hardenable diameter when its concentration is above 1-wt%. Moreover, nickel together with manganese, is the only alloying element that has the unique ability of simultaneously increasing hardenability, strength, and toughness (Davis, 2001; Narasimha Rao & Thomas, 1980) with little penalty on weldability, as explained in Section 3.5.

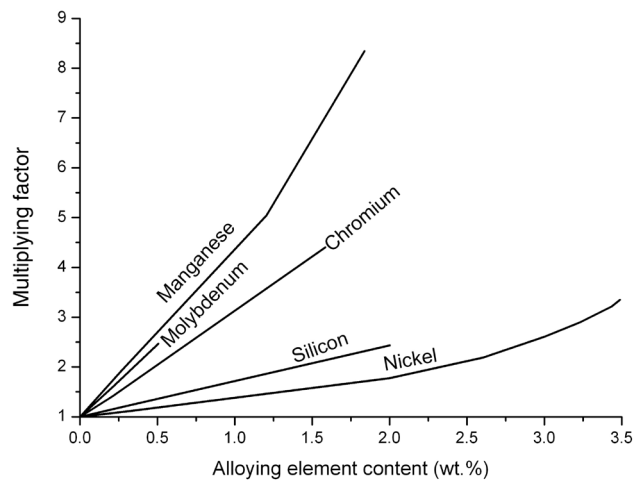


Figure 1 Multiplying factors for common alloying elements in LASs (Krauss, 2005a).

Reprinted with permission of ASM International. All rights reserved. www.asminternational.org.

Nickel does not form carbides and therefore delays proeutectoid ferrite, pearlitic, and bainitic reactions (Siebert et al., 1977). Transformation-temperature-time (TTT) curves can be used to illustrate the effect of alloying elements on retarding diffusion-assisted transformations. Figure 2 shows the effect of nickel on TTT curves by comparing nickel-free UNS G41400 (SAE/AISI 4140) steel vs. UNS G43400 (SAE/AISI 4340), a nickel-containing LAS of similar composition. As seen in Figure 2, Ni has a marked effect on transformation kinetics. A 1.79-wt% Ni addition delays the nose of the ferritic/pearlitic transformation by approximately 100 s (Vander Voort, 1991). Likewise, nickel caused a shift of 8 s in the bainite nose. Upper bainite is an undesirable microstructure due to its poor combination of strength and toughness, associated with the precipitation of carbides between ferrite laths (Krauss, 2005b). Figure 2 also shows that upper bainite finish temperatures are displaced to longer times. Nickel also delays the position of ferrite start and bainite start reactions on continuous cooling transformation diagrams (Garber, 1983). A 1-wt% Ni addition to a Mo-Nb-modified UNS G43400 (SAE/AISI 4340) steel resulted in an increase in ferrite start time of about 5000 s, whereas the bainite start time was displaced by about 300 s.

Given that there is certain degree of synergy between different alloying elements, the addition of several elements in small amounts has a more pronounced effect on hardenability than the use of fewer elements in higher concentrations (Kuch, 1990; Mukerjee, Mediratta, & Ramaswamy, 1986; Scoonover & Arnson, 1984). In this regard, ideal diameter calculations based on Equation 6 give only a rough preliminary approximation because the actual

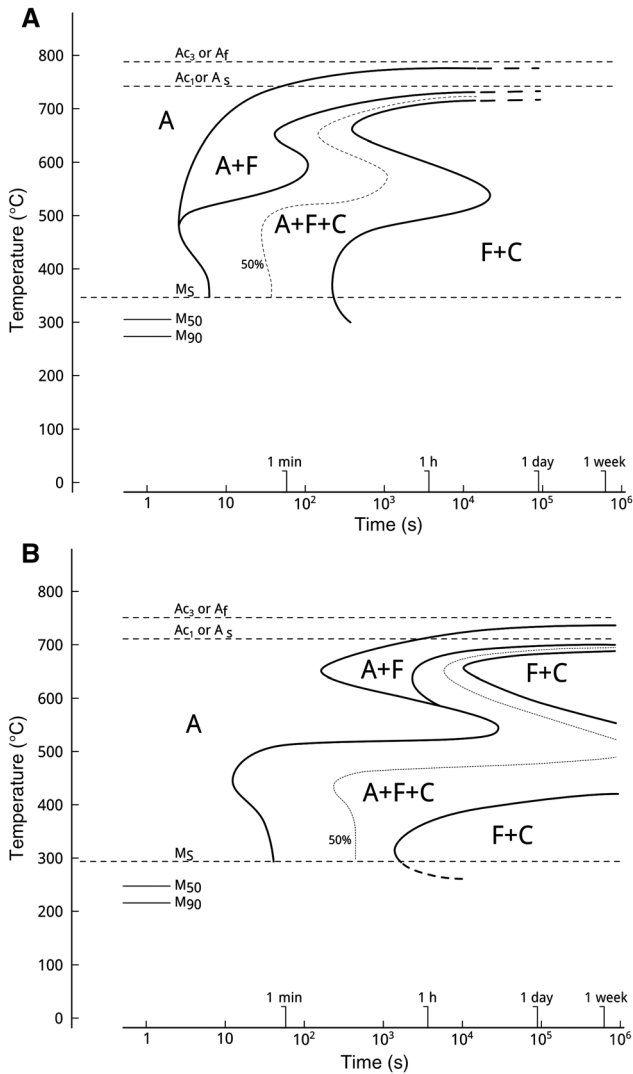


Figure 2 TTT curves for (A) UNS G41400 (SAE/AISI 4140) steel (0.37-wt% C, 0.77-wt% Mn, 0.98-wt% Cr, and 0.21-wt% Mo) and (B) UNS G43400 (SAE/AISI 4340) steel (0.42-wt% C, 1.79-wt% Ni, 0.78-wt% Mn, 0.80-wt% Cr, and 0.33-wt% Mo), showing the effect of Ni on phase transformation kinetics, after Vander Voort (1991). A, austenite; F, ferrite; C, cementite. M50 and M90 indicate the temperature at which austenite is half transformed and 90% transformed to martensite, respectively. Reprinted with permission of ASM International. All rights reserved. www.asminternational.org.

effect of a given element is influenced by the concentration of other alloying elements. For example, the presence of 1-wt% Ni increases the multiplication factor of Mo from 3 to 3.9, at 1-wt% Mo (DeRetana & Doane, 1971). Thus, in practice, Ni is always used in combination with Mo, Mn, and Cr. Increasing Mn, Cr, or Ni, in combination with Mo, suppresses the start of the bainitic reaction in low- and medium-carbon steels (Scoonover & Arnson, 1984).

Several authors (Garber, Wada, Fletcher, & Cox, 1985; Jarvis & Bulloch, 1992; Yoshino & Minozaki, 1986)

have suggested that Ni additions become essential as the thickness of wellhead parts increases. Moreover, common Cr-Mo steels cannot be heat treated to a homogeneous through-thickness structure in the absence of Ni (Garber et al., 1985; Jarvis & Bulloch, 1992; Yoshino & Minozaki, 1986). This is best illustrated in Figure 3 by comparing the Jominy curves of UNS H43400, which contains approximately 1.8% Ni, and nickel-free UNS H41400 (Jatczak, 1978). The suffix “H” in the UNS/SAE designation indicates that the steel has hardness requirements so that the curve of “hardness vs. distance from the quenched end” falls inside the band limited by the minimum and maximum hardenability values (Figure 3). Figure 3 shows that the hardness from the quenched end falls in a steeper fashion for UNS H41400 than for UNS H43400, which highlights the effect of nickel on hardenability.

3.4 Effect of nickel in fracture toughness

Nickel’s effect on through-thickness hardenability results in improved fracture toughness (Schillmoller & Craig, 1987). Nickel increases low-temperature fracture toughness (Davis, 1990, 2001) by refining ferrite grains and changing the inherent mechanical properties of ferrite. For example, a 3.3-wt% Ni addition to a fully annealed Fe-0.03-wt% C alloy resulted in a decrease in DBTT of 70°C (i.e., from 10°C to -60°C) and a slight increase in the upper shelf energy (Jolley, 1968a).

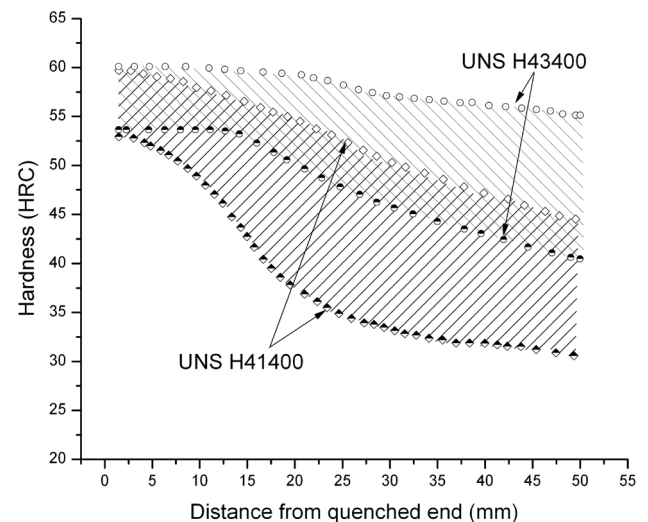


Figure 3 Jominy curves for UNS H41400 (SAE/AISI 4140H) and UNS H43400 (SAE/AISI 4340H) (as indicated), showing the effect of nickel on hardenability (Jatczak, 1978). Reprinted with permission of ASM International. All rights reserved. www.asminternational.org.

Jolley (1968a) showed that while Mn additions decreased the DBTT of a Fe-C alloy, Mn alone did not change the DBTT of decarburized iron, suggesting a mechanism based on the refining of grain boundary carbides (Jolley, 1968a). In contrast, nickel additions lowered DBTT regardless of carbon content (Jolley, 1968a,b; Leslie, Sober, & Babcock, 1969). These Ni-containing LAS were heat treated to yield ferrite or a ferrite solid solution of about 3-wt% Ni, suggesting an improvement in the inherent properties of the ferrite phase rather than the presence of second-phase particles or changes in carbide shape or distribution (Jolley, 1968a).

To explain the increased fracture toughness of Ni-containing ferrite, Jolley (1968b) and Leslie et al. (1969) suggested that nickel favors cross-slip, i.e., the ability of screw dislocations to move in any plane that contains their Burgers vector (Dieter, 1986), at cryogenic temperatures and high strain rates. Petch (1987), meanwhile, proposed a mechanism based on alloy softening at low temperatures and high strain rates. In addition, nickel contributes to grain size refinement (Davis, 2001; Jolley, 1968a), which also lowers the DBTT (Roe & Bramfitt, 1990).

By its indirect effect on reducing both A_c1 and M_s , nickel can lead to retained austenite (Davis, 2001). As explained in Section 3.1, the presence of retained austenite is often detrimental because it can lead to untempered martensite. However, retained austenite is necessary for extreme low-temperature applications where DBTT as low as -200°C are required (Campbell, 2008). In this regard, steels with 5-wt% Ni can be heat treated to yield a microstructure consisting of lath martensite with fine retained austenite films in prior austenite grain boundaries (Narasimha Rao & Thomas, 1980) or austenite with ferrite and tempered martensite (Sarno, Bruner, & Kampschaefer, 1974). The effect of retained austenite is therefore beneficial in terms of fracture toughness because the entire “absorbed energy vs. temperature” curve shifts upward toward higher energies, accompanied by a decrease in DBTT (Narasimha Rao & Thomas, 1980).

Steels for ultralow-temperature and cryogenic applications conform to, e.g., ASTM A320/A320M, A333/A333M, A352/A352M, A353, A553, A645, and shall meet minimum CVN impact energy requirements. For example, whereas 9-wt% Ni-steels shall have a 27-J minimum CVN energy at -195°C (ASTM, 2014), 4–5-wt% Ni-steels shall retain high CVN impact toughness values down to -160°C (ASTM, 2010b). Various 3.5-wt% Ni-steels were successfully used in sour refinery environments for many years, in applications requiring good low-temperature impact toughness (Bush, Brown, & Lewis, 2004).

Lower nickel-containing steels, such as UNS G43400 (SAE/AISI 4340), have interlath-retained austenite when

quenched and tempered at temperatures up to 250°C (Malakondaiah, Srinivas, & Rama Rao, 1997). A tempering temperature in the 200°C – 250°C range is considerably lower than recommended tempering temperatures for high-strength steels for O&G applications. Interlath-retained austenite in UNS G434000 (SAE/AISI 4340) also increases fracture toughness (Zhirafar et al., 2007). Proposed mechanisms for the improved fracture toughness with retained austenite include promotion of crack branching, crack blunting due to plastic flow in retained austenite, prevention of interlath boundary carbide precipitation, and transformation-induced plasticity, where retained austenite transforms to martensite at the crack tip, relieving stress concentration (Malakondaiah et al., 1997; Narasimha Rao & Thomas, 1980).

For sweet (i.e., for environments free of H_2S ; EFC, 2009) O&G applications, toughness of, e.g., UNS G43400 (SAE/AISI 4340), is seldom increased by precipitation of retained interlath austenite. As-quenched UNS G43400 (SAE/AISI 4340) steels are typically tempered in the 600°C – 700°C (but below A_c1) range (Payer et al., 1986; VGS, 2012a, 2013a), where retained austenite becomes destabilized and transforms to fresh martensite upon cooling. Because hardness is limited to a maximum of 35-HRC (DNV, 2010; ISO, 2010b) to prevent HE due to cathodic protection, a second heat treatment is often mandated to temper the fresh martensite. For sour service, a similar requirement, but with a 22-HRC limit, should apply when evaluating LAS with a Ni content above the 1-wt% maximum established by ISO 15156-2.

3.5 Effect of nickel on weldability

Empirical CE expressions have been developed to quantify the effect of the main alloying elements on weldability relative to carbon. CE expressions are based on the effect of alloying elements on the hardness of the heat-affected zone (HAZ), end of transformation temperature, the HAZ toughness, and/or cold cracking resistance (Grong & Matlock, 1986). Generally, as carbon content increases, so does the hardness at the expense of toughness and increased cold cracking susceptibility (Bryhan, 1981).

Cold cracking is a form of HE, where hydrogen absorbed during the welding process generates cracks in a susceptible microstructure with applied or residual stresses. The amount of untempered martensite, which is considered the most susceptible microstructure to HE, increases as CE increases (Snape, 1968b). Thus, steels with higher CE values are more susceptible to cold cracking than leaner chemistries.

The two most common CE expressions used by most design codes and standards are (API, 2007; NORSOK, 2010):

$$\text{For } C \leq 0.12\text{-wt\%: CE(Pcm)} = C + \frac{\text{Si}}{30} + \frac{\text{Mn}}{20} + \frac{\text{Cu}}{20} + \frac{\text{Ni}}{60} + \frac{\text{Cr}}{20} + \frac{\text{Mo}}{15} + \frac{\text{V}}{10} + 5B \quad (7)$$

$$\text{For } C > 0.12\text{-wt\%: CE(IIW)} = C + \frac{\text{Mn}}{6} + \frac{(\text{Cr} + \text{Mo} + \text{V})}{5} + \frac{(\text{Ni} + \text{Cu})}{15}, \quad (8)$$

whereas the CE formula proposed by the International Institute of Welding (IIW), Equation 8, works very well for C-Mn steels with a carbon content above 0.12-wt%, the CE(Pcm) formula, or the Ito-Bessyo expression (API, 2007), Equation 7, has been shown to be more appropriate for low-carbon micro-alloyed steels (Gordine, 1977). In all cases, Ni is multiplied by a coefficient smaller than other common alloying elements such as Cr, Mo, Si, V, and Mn (Bryhan, 1981; Grong & Matlock, 1986; Lancaster, 1997; Yurioka, Suzuki, Ohshita, & Saito, 1983). Thus, nickel additions carry a lower penalty in terms of weldability. However, it has been criticized that for low-carbon, high-strength low-alloy steels (HSLA), there is poor correlation between hardness and cold cracking resistance with any of the commonly used CE equations (Bryhan, 1981). Nevertheless, the same author (Bryhan, 1981) concluded that the cold cracking susceptibility was independent of nickel content.

In general, increasing the degree of alloying of the base metal leads to higher hardness in the HAZ. The increase in hardness is due to the effect of alloying elements on hardenability and to the temperature-time profile experienced by the material in the HAZ. For example, additions of Ni and Cr above 2.8 and 1.3-wt%, respectively, lead to the formation of martensite in the HAZ, which impacts fracture toughness negatively (Eroğlu, 2002). For a given degree of alloying, a higher heat input can lead to a lower cooling rate and less amount of martensite in the HAZ (Eroğlu, 2002; Eroglu & Aksoy, 2002). However, excessive heat inputs can reduce fracture toughness due to coarsening of austenite grains (Eroğlu, 2002).

Interestingly, the nickel limit on welding consumables imposed by ISO 15156-2 is not as restrictive as the one imposed to the base metal (NACE-ISO, 2001). Welding consumables and procedures that produce deposits with more than 1-wt% Ni are permitted after successful SSC qualification in accord with the standard. In this regard, weld consumables with over-matching nickel content are necessary to obtain a higher strength on the weld seam

than on the base metal. Other standards such as the European Federation of Corrosion Publication No. 16 (EFC 16) (EFC, 2009) and the now discontinued NORSOK M-002 are even less restrictive than ISO/NACE. Based on results presented by Gooch (1982a, b), EFC 16 suggests that welding consumables with a maximum Ni content of 2.2-wt% improve fracture toughness without negatively impacting SSC resistance. Gooch (1982a, b) conducted hydrogen absorption and SSC tests on weld metal containing up to 2.2-wt% Ni and concluded that Ni *per se* did not have a consistent negative impact on SSC resistance.

As shown in Section 3.1, Ni as well as Mn stabilizes austenite and lowers the transformation temperature of austenite to ferrite (Grong & Matlock, 1986), i.e., A_{c1} . Nickel also retards the nucleation and growth kinetics of grain boundary ferrite (Grong & Matlock, 1986; Wang & Liu, 2002), refining the microstructure and increasing the proportion of acicular ferrite in welded structures at the expense of pro-eutectoid or grain boundary ferrite (Zhang & Farrar, 1997). Given their small grain size, typically in the 1- to 3- μm range, and high-angle grain boundaries, welds with a high volume fraction of acicular ferrite show an optimal combination of strength and toughness (Bhole, Nemade, Collins, & Cheng, 2006; Grong & Matlock, 1986; Wang & Liu, 2002; Zhang & Farrar, 1997). As a result, Ni lowers the DBTT in weld deposits (Zhang & Farrar, 1997), similar to its effect on the base metal.

The optimal nickel content to obtain the highest impact toughness depends on the amount of other alloying elements, specially Mn (Wang & Liu, 2002; Zhang & Farrar, 1997) and Mo (Bhole et al., 2006). For example, whereas maximum toughness for 1.6-wt% Mn is obtained at 1-wt% Ni, 0.7-wt% Mn requires 2.5–3.5-wt% Ni (Zhang & Farrar, 1997). At the optimal Mn-to-Ni ratio, the microstructure consists of a high volume fraction of acicular ferrite, with some pro-eutectoid ferrite and a minimum amount of martensite and segregation (Zhang & Farrar, 1997). Manganese and/or nickel additions beyond the optimum level can lead to increased amounts of martensite and segregation, which negatively impacts the fracture toughness of the weld. Furthermore, a post-weld heat treatment is required unless fresh martensite is tempered by reheating during subsequent passes (Snape, 1968b).

4 Effects of nickel on sour service performance of LAS

Despite significant efforts, the effects of Ni on SSC susceptibility remain unclear to date. Several authors (Biagiotti,

1995; Snape, 1968; Payer et al., 1986) stated that Ni does not affect SSC resistance unless susceptible phases, such as untempered martensite, are present in the final microstructure. Others (Dunlop, 1978; Craig et al., 1990; Kaneko & Ikeda, 1988; Yamane et al., 1986; Yoshino & Minozaki, 1986) have shown an increase in surface trenching in Ni-containing steels exposed to sulfide-containing solutions. Surface trenches could in turn act as crack initiation sites, especially in parts with few geometric stress concentrators. In threaded tubular products, meanwhile, threads provide favorable sites for crack nucleation (Garber, 1983), so it is the resistance to crack propagation rather than crack initiation that becomes critical to determine the integrity of the structure.

LAS have been traditionally restricted by ISO 15156-2 to Ni contents below 1.0-wt% on the assumption that higher Ni concentrations could negatively affect SSC resistance. This has a direct impact on commercial nickel-containing LAS including UNS G43XX0 and UNS G46XX0 (formerly SAE/AISI 43XX and 46XX), 30CrNiMo8 (EN 1.6580), 36NiCrMo16, and 33NiCrMoV14-5 (EN 1.6956), which have outstanding hardenability and can be heat treated to a high toughness (Payer et al., 1986).

The limitation suggested by ISO and NACE is mostly based on a body of research conducted during the 1960s and 1970s (Dunlop, 1978; Treseder & Swanson, 1968). In their pioneer work, Treseder and Swanson (1968) and Dunlop (1978) found that LAS with more than 1.0-wt% Ni were more susceptible to SSC under similar loading and environmental conditions. Treseder and Swanson reported that steels with a Ni content higher than 1.0-wt% were susceptible to SSC even if hardness was kept under 235-BHN, which is equivalent to the 22-HRC limit now adopted by ISO 15156-2. Treseder and Swanson and Dunlop based their conclusions on the NACE TM 01777 Method B (referred to as Shell bent-beam test at that time; NACE, 1996) where a beam is bent at constant deflection with two holes that act as stress raisers in the centerline (Fraser, Eldredge, & Treseder, 1958). A constant displacement is imposed on the beam, and it is then immersed in 0.5-wt% acetic acid solution saturated with H_2S for 30 days. The acceptance criteria established by the O&G industry mandates no cracks after testing. However, Snape (1968a) criticized Treseder and Swanson's results, suggesting that the A_{c1} temperature had been exceeded during heat treatment leading to the presence of untempered martensite, which negatively affects SSC resistance (Snape, 1968b). Furthermore, Snape criticized the excessive stress imposed by the stress concentrator sites, suggesting that based on elasticity theory, the calculated real maximum applied stress may have exceeded the UTS of the material five times.

Therefore, plastic deformation inevitably occurred close to the stress concentrators.

In recent years, O&G companies have abandoned the NACE TM0177 Method B test in favor of the four-point bent-beam approach. The four-point bent-beam method is a constant displacement test performed by supporting a smooth beam specimen with no stress concentrators on two loading rollers and applying a load through two other loading rollers. This configuration leaves the outer face of the specimen in tension and the inner one in compression (EFC, 2009; Total, 2005b). Although NACE TG085 is currently developing a four-point bent-beam procedure that will be ultimately incorporated in a revised version of the TM0177 specification (NACE, 2014), no systematic studies on the effect of Ni on SSC resistance have been conducted using this test method.

In later studies, several researchers have found conflicting evidence, most of them finding no correlation between SSC performance and nickel content. Craig suggested that the early work on SSC of nickel steels did not control other metallurgical variables well enough to draw a conclusion about possible deleterious effects by nickel (Craig, 1988). Payer et al. studied the effects of different heat treatments on the SSC performance of nickel steels with nickel contents ranging from 0 to 3-wt% (Payer et al., 1986). The authors found that under the correct heat treatment conditions all steels had adequate SSC resistance. Nevertheless, only a double tempering treatment rendered the higher nickel LAS resistant to SSC.

Because Ni lowers A_{c1} and imparts some degree of solid solution strengthening, the required tempering temperature could be close to or above A_{c1} . If A_{c1} is exceeded on the first temper, some martensite can transform back to austenite first and to untempered martensite upon cooling, which may lead to exceeding the 22-HRC/250-HV hardness limit imposed by ISO 15156-2. The risk of exceeding A_{c1} is greatest in segregated areas with higher content of alloying elements (Craig et al., 1990). Ni tends to aggravate this problem because it has a tendency to segregate during solidification (Yoshino & Minozaki, 1986). In those cases, a second temper to transform the entire microstructure to tempered martensite is required (Craig et al., 1990; Snape, Schaller, & Forbes Jones, 1969; Payer et al., 1986), which is the desired microstructure to obtain the highest SSC resistance (Snape, 1968b). Furthermore, Snape et al. (1969) has suggested that the resultant microstructure after the dual temper heat treatment, consisting of patches of coarse and fine carbides in a ferritic matrix, combined high YS values (107-ksi) with superior SSC resistance.

Double tempering does impose an economic penalty over single heat treatment procedures. However, double

tempering is not an uncommon practice in the O&G industry and it is rendered mandatory in high-strength LAS for heavy-wall components (VGS, 2012d). Nevertheless, other authors have reported that for UNS G43400-type steels with nickel contents below 2-wt%, a single temper 40°C below A_{c1} could result in hardness values under 22 HRC and an SSC resistance similar to that of Ni-free steels (Biagiotti, 1995).

The rest of this section reviews the effect of microstructure on SSC performance, the effect of Ni on hydrogen transport properties, the effect of plastic deformation on SSC resistance, and the role of nickel on pitting/trenching. The section ends with a discussion on proposed SSC mechanisms.

4.1 Effects of microstructure

Regardless of their Ni content, the SSC resistance of LAS seems to be more microstructure related than composition related. Snape (1967) found that the resistance to cracking of LAS decreased as the strength increased. Above 29 HRC, all LAS failed by SSC independently of their Ni content. Snape's research into the effects of composition and microstructure on the SSC susceptibility of LAS also indicated that untempered martensite, originating when tempering around the A_{c1} temperature, drastically lowered SSC resistance (Snape, 1968b). Therefore, it seems plausible to assume *a priori* that a LAS composition leading, after proper heat treatment, to tempered martensite (or to complete lower bainite as discussed below) could result in better SSC performance irrespective of its Ni content. In this regard, no detrimental effect of nickel was observed during SSC testing of properly heat treated LAS, covering a wide 600- to 1400-MPa (90–200-ksi) YS range (Snape, 1967).

A quenched and tempered microstructure with fine spheroidized carbides uniformly distributed in ferrite presented a greater SSC resistance than a normalized and tempered structure of the same strength level (Snape, 1967, 1968b). Normalized and tempered microstructures or other microstructures obtained during isothermal transformation exhibited coarser globular or lamellar carbides, which are more susceptible to SSC than the more refined microstructures obtained after quenching and high-temperature annealing (Snape, 1968b). The steels with the poorest SSC resistance were those that contained untempered martensite (Payer et al., 1986; Snape, 1968b). In contrast, Yoshino and Minozaki (1986) determined that a small volume fraction of untempered martensite, on the order of ~5%, had no detrimental effect on SSC resistance. Nevertheless, both authors concluded that SSC resistance,

for a given microstructure and strength level, was independent of Ni content (Snape, 1968b; Yoshino & Minozaki, 1986).

Craig et al. (1990) proposed that the decrease in M_s caused by Ni could influence the type of martensite that forms upon cooling. Snape (1967) proposed that plate or twinned martensite was more susceptible to SSC than lath martensite; however, this type of martensite was found by the author for steels with Mn or Ni in the order of 8%. LAS with carbon higher than 0.6-wt% can present twinned martensite upon quenching as well. However, on low- and medium-carbon LAS, the M_s is usually above the 315°C threshold for plate martensite formation (Krauss, 2005a). Thus, low- and medium-carbon LAS should consist of lath martensite exclusively. In particular, for the laboratory-grade Ni-modified SAE/AISI 4130 steels with up to 3.7-wt% Ni studied by Craig et al., the minimum M_s calculated using Equation 3 was approximately 328°C, which is above the threshold for plate martensite formation.

4.1.1 The role of retained austenite

It was previously discussed that due to the effect of nickel on decreasing A_{c1} and M_s , nickel alloy steels could present retained austenite in the final microstructure. Retained austenite has a larger hydrogen solubility than ferrite, but hydrogen diffusivity is about two orders of magnitude slower (Solana, Takamada, Bernstein, & Thompson, 1987). The effect of retained austenite on HE is a function of the amount, distribution, and mechanical stability of the compact face centered cubic (fcc) phase. In this context, mechanical stability refers to the stability to martensite transformation upon application of plastic strain, which is gauged by the martensitic deformation temperature, M_d . Retained austenite, if present as a mechanically stable continuous film, could act as a barrier for hydrogen diffusion (Solana et al., 1987). However, crack tip opening displacements are typically large enough to cause fracture of retained austenite films. This effect is therefore not expected to increase cracking resistance significantly (Solana et al., 1987).

Snape (1967) suggested that steels with retained austenite could exhibit increased SSC resistance. However, his conclusions were made after analyzing austenite volume fractions on the order of 30%–90%, which are unlikely to be encountered in quenched and tempered LAS. LAS have a much lower amount of retained austenite, and there is danger that it could transform to fresh martensite upon cold work. Solana et al. (1987) argues that this transformation consumes elastic energy, reducing the driving force

available at the crack tip, so that a higher stress intensity is required to increase crack growth. However, due to the higher hydrogen solubility in austenite vs. ferrite or martensite, hydrogen is released into the bcc lattice during this transformation. Other authors (Kim, Kim, & Morris, 1986) indicated that due to the volume expansion caused in the transformation of the compact to the non-compact martensite phase, a tensile stress is imposed in the lattice, which contributes to crack propagation. Solana et al. (1987) and Kim et al. (1986) conclude that retained austenite had no beneficial effect on hydrogen-assisted cracking resistance. In other words, any positive effect in terms of hydrogen solubility is offset by retained austenite mechanical instability, with possibility of hydrogen release and increase in the triaxial state of stress in the crack zone.

When cracking proceeds intergranularly aided by segregation of impurities to grain boundaries, the presence of retained austenite could, in fact, increase HE resistance (Lessar & Gerberich, 1976). This is a special case where austenite acts as a scavenger of impurities (Kim et al., 1986), reducing the concentration of deleterious elements at grain boundaries. However, the best engineering practice to improve toughness and reduce the risk of an SSC failure is to minimize the amount of retained austenite and grain boundary impurities (Kim et al., 1986).

4.1.2 Bainite resistance to SSC

Nickel, when combined with Mn, Cr, and Mo, has the ability to suppress the start of the ferritic and bainitic reactions (Garber, 1983; Scoonover & Arnson, 1984), Figure 2. Bainite is an acicular ferrite-cementite microconstituent, and the result of a diffusion-assisted austenite transformation (Krauss, 2005b). Bainite is classified based on transformation temperature as upper or lower bainite. Although the actual transformation temperature depends on carbon content, upper bainite dominates over ferritic-pearlitic microstructures below approximately 500°C, whereas lower bainite is the prevailing microstructure below 300°C (Krauss, 2005b).

Upper bainite is characterized by carbides growing between ferrite laths due to carbon rejection in growing ferrite crystals. In lower bainite, carbides are retained inside the ferrite lath due to the increased undercooling and slower diffusion rate. Owing to the finer distribution of carbides obtained at lower temperature, lower bainitic steels generally exhibit higher strength, ductility, fracture toughness, and lower DBTT than upper bainitic steels (Krauss, 2005b).

In the subsea O&G industry, bainitic high-strength LAS with a nickel content ranging from 0.75% to 1% are commonly used for hub and cap as well as pup and transition piece forgings for low-temperature service (VGS, 2012c, 2013a,b). It is important, therefore, to understand the sour service performance of such steels.

Garber (1983) studied the effect of different cooling rates on the microstructures of laboratory grade steels, based on UNS G41300 (SAE/AISI 4130) alloy modified with Ni-Mo-Nb. The severity of quenching was selected to yield either fully martensitic or fully bainitic microstructures. The critical stress intensity factor for sulfide stress cracking, KI-SSC, K_{I-SSC} of fully martensitic microstructures tempered to strength levels in the 620- to 725-MPa range were 56 and 40-MPa·m^{1/2}, whereas fully tempered bainitic microstructures with similar YS gave K_{I-SSC} values between 42 and 32-MPa·m^{1/2} (Garber, 1983). Similar results were presented by Asahi, Sogo, Ueno, and Higashiyama (1989) for steels quenched and tempered to a 750-MPa YS having a martensitic microstructure with different volume fractions of upper bainite, ranging from 3- to 40-vol%. A 40-vol% upper bainite in a tempered martensite microstructure resulted in a decrease in K_{I-SSC} from 50 to 40 MPa·m^{1/2}. Likewise, Grobner, Sponseller, and Diesburg (1976) investigated UNS G41350 (SAE/AISI 4135) steels quenched at different cooling rates to yield fully martensitic, martensitic+bainitic, and fully bainitic microstructures with a 720-MPa SMYS. In line with Garber and Asahi et al., the author showed that a fully tempered martensitic microstructure had a critical strain, as determined by the NACE TM0177 Method B bent-beam method, that was approximately 67% higher (0.70 vs. 0.42, respectively) than that of a fully bainitic steel.

Other authors (Dvoracek, 1970; Hudgins, McGlasson, Mehdzadeh, & Rosborough, 1966; Snape, 1968b) concluded that, at the same YS, normalized and tempered LAS underperformed quenched and tempered counterparts. Although not explicitly mentioned by the authors, it is plausible to assume, given the dimensions of the samples and the degree of alloying, that the microstructure of normalized and tempered steels had a significant fraction of upper and lower bainite (Sponseller, Garber, & Straatmann, 1982). In other words, at the same YS, quenched and tempered martensitic steels had a better SSC resistance than tempered bainitic steels.

Yoshino (1982), in contradiction to most authors, claimed that upper and lower bainitic steels had a higher SSC threshold stress, σ_{th-SSC} , than quenched and tempered steels in the range of 700–800 MPa. In his study, LAS were quenched at a rate that simulates the 1/4 thickness position of 100-mm-thick water-quenched steels.

Transformation start temperature, i.e., the temperature at which the γ/α transformation begins, was determined as a function of Cr content. The authors reported a decrease in σ_{th-SSC} , from 500 to 200 MPa, as the transformation temperature decreased from 500°C to 300°C due to an increase in Cr. This suggests, the authors concluded, that upper bainitic microstructures had a better SSC resistance than tempered martensitic ones. However, the experimental design used by the authors did not allow them to separate the effect of microstructure on SSC resistance from that of the Cr content of the alloys. Furthermore, a comparison of Yoshino's (1982) σ_{th-SSC} vs. YS curves on bainitic LAS of a wide range of composition with similar correlations presented by Snape (1968b) for quenched and tempered steels (Figure 4) suggests that, for a given strength level, quenched and tempered steels offered the highest SSC resistance. The figure also shows that normalized and tempered steels underperform quenched and tempered steels. Owing to the addition of alloying elements, it is likely that those normalized and tempered steels had a bainitic microstructure (Sponseller et al., 1982), explaining why those points fall inside the scatter band of bainitic steels studied by Yoshino. Steels with untempered martensite studied by Snape (1968b) had the lowest SSC resistance.

The reasons for bainitic microstructures underperforming martensitic microstructures in SSC tests are not discussed in depth in the literature. Furthermore, most authors make no distinction between the type of bainite

present in the steel and do not quantify the upper bainite-to-lower bainite ratio. Grobner et al. (1976) suggested that differences in hydrogen transport between bainite and martensite, higher segregation of impurities at lower cooling rates, and bainite's more heterogeneous microstructure could all play a role. Other authors suggested that the bainite-ferrite boundary in low-carbon steels is a favorable site for crack nucleation (Kimura et al., 1989). Differences in carbide distribution, according to Yoshino (1982), caused differences in hydrogen absorption and trapping. Yoshino (1983) concluded that interlath carbides in as-cooled upper bainite absorb much more hydrogen than interlath carbides in as-cooled lower bainite (i.e., from approximately 16 ppm down to 5 ppm, respectively). Based on HE trap theory (Pressouyre, 1980), it is plausible to assume that upper bainite should have lower SSC resistance due to the presence of coarse carbides precipitated preferentially at lath boundaries. However, this conclusion may be questionable for tempered structures, given that both microstructures absorbed a similar amount of hydrogen after tempering at 600°C (Yoshino, 1983).

To assure adequate weldability of heavy sections, the amount of carbon and other alloying elements is typically limited to CE(IIW) values in the 0.42–0.48 range (AWS, 2002; DNV, 2012; Total, 2005a; VGS, 2012c), which places a limitation on hardenability as well. Therefore, the presence of bainite in the microstructure becomes inevitable as the thickness of the section increases (Garber et al., 1985; Yoshino, 1982), which cannot be quenched at

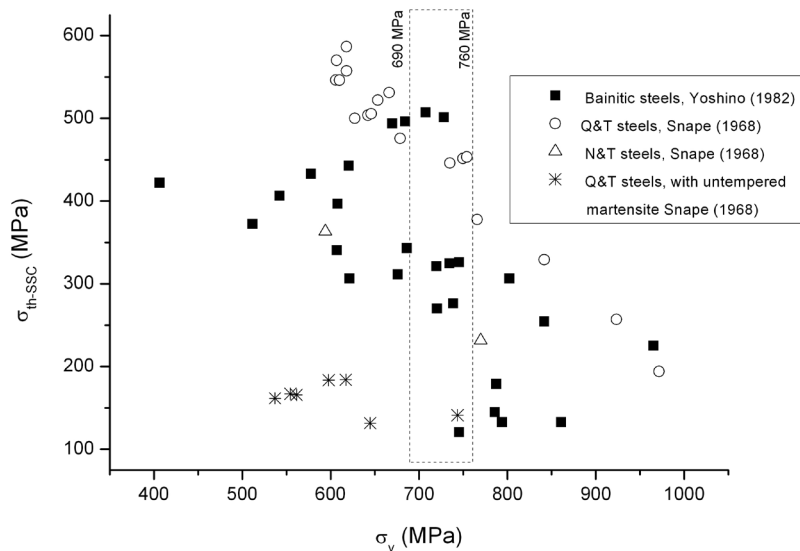


Figure 4 Threshold stress for SSC vs. YS for LASs, comparing the effect of microstructure on SSC resistance, adapted from Snape (1968b) and Yoshino (1982).

Dashed lines indicate the typical SMYS range for nickel alloy steels compliant with ISO 15156-2 requirements, with permission of © NACE International, 1982, 1968.

cooling rates higher than the critical. As discussed above, Ni additions improve hardenability and increase the amount of bainite over that of less desirable microstructures (i.e., as ferrite and pearlite) (Carneiro, Ratnapuli, & Freitas Cunha Lins, 2003; Garber et al., 1985), with a low penalty on weldability.

4.2 Effect of nickel on hydrogen absorption, diffusion, and trapping

Crack growth at high H_2S contents is a process controlled by hydrogen absorption (Asahi, Ueno, & Yonezawa, 1994; Berkowitz & Heubaum, 1984; Kawashima, Hashimoto, & Shimodaira, 1976; Snape, 1967; Turn, Wilde, & Troianos, 1983). Hydrogen absorption rates are commonly determined by analyzing steady-state hydrogen permeation current density transients using the Devanathan and Stachurski cell (Devanathan & Stachurski, 1962). The steady-state hydrogen permeation of a steel in a given environment is a measure of the amount of diffusible hydrogen that can be absorbed. As shown by several authors, the ductility and reduction in area, as measured using slow strain rate testing (SSRT), decreased with an increase in the steady-state hydrogen permeation rate (Berkowitz & Heubaum, 1984; Saenz de Santa Maria & Turnbull, 1989; Turn et al., 1983). Likewise, SSC performance, as determined by constant load testing, decreased with an increase in hydrogen permeation rate due to a decrease in pH or an increase in H_2S concentration (Asahi et al., 1994). Other authors studied the amount of hydrogen absorbed in a given environment by vacuum hot extraction or the inert fluid displacement method. As the amount of hydrogen absorbed increased by a decrease in pH or an increasing cathodic current, the time to failure at constant load (Snape, 1967) and the performance in an SSRT (Kawashima et al., 1976) decreased accordingly. Likewise, as the diffusible hydrogen content increases, the threshold stress intensity for hydrogen cracking decreases (Gangloff, 2003; Gerberich & Chen, 1975). Therefore, if Ni had any effect on promoting hydrogen absorption, Ni additions could potentially translate into a lower SSC resistance.

Ni affects hydrogen transport directly by H-Ni interactions and indirectly by changes in the microstructure (Pressouyre, 1979). These interactions can be quantified by the effect of nickel on the trap affected or effective hydrogen diffusion coefficient, D_{eff} (Oriani, 1970). Traps are special sites in the lattice with a hydrogen dissolution enthalpy that is energetically favorable relative to ordinary sites (Hirth, 1980; Oriani, 1970). Trapping sites in steels include alloying elements in solid solution, dislocations,

carbides, inclusions, and second-phase interfaces and microcracks, which can develop during cold work (Hirth, 1980; Oriani, 1970). Traps slow down hydrogen diffusivity because of the longer residence time when compared with a normal interstitial site (Turnbull, Carroll, & Ferriss, 1989). In this regard, there are two types of traps: (i) irreversible and (ii) reversible traps. A trap is considered irreversible if trapped hydrogen will not desorb at the testing temperature. In contrast, hydrogen can diffuse out of a reversible trap when sufficient energy is administered to the system. In a lattice with traps that contain hydrogen below its equilibrium amount, Fick's law no longer applies and a different differential equation has to be used to solve the transport equations, as discussed elsewhere (Mc Nabb & Foster, 1963; Turnbull, Saenz de Santa Maria, & Thomas, 1989).

D_{eff} is typically used to describe hydrogen transport in presence of traps. When inserted into Fick's first law, D_{eff} relates the observed flux with the total hydrogen concentration, which is defined as the sum of contributions from lattice and trapping sites (Oriani, 1970). Use of D_{eff} is limited to cases where (i) irreversible trapping is not observed, (ii) the fraction of traps occupied is low, and (iii) hydrogen in lattice and trap sites is at equilibrium (Turnbull, Carroll, & Ferriss, 1989). In those cases, use of D_{eff} can give an estimate of the charging time required to saturate a fracture mechanic or tensile test specimen or structural component with hydrogen. In contrast to the conventional or lattice diffusion coefficient, D_{eff} is a function not only of temperature, but also of hydrogen concentration in normal and trap sites (Oriani, 1970; Turnbull, Carroll, & Ferriss, 1989). Numerically, D_{eff} is smaller than the lattice diffusion coefficient because it takes into account interactions with trap sites. However, as discussed by Turnbull, Carroll, & Ferriss (1989), irreversible trapping cannot be neglected in carbon and LASSs. Furthermore, the trap occupancy factor is likely high in environments containing H_2S . In addition, D_{eff} commonly increases during a hydrogen permeation test (Kappes et al., 2012; Turnbull, Saenz de Santa Maria, et al., 1989) due to an increased concentration of hydrogen in traps (Oriani, 1970).

A steady-state hydrogen concentration is likely to be reached when measuring K_{I-SSC} , σ_{th-SSC} , or the critical stress to failure in the bent-beam specimens, S_c , if hydrogen transport by dislocations can be neglected. Those tests, standardized as NACE Method D, A, and B, have a duration of 14 days (Method D) or 30 days (Methods A and B) (NACE, 1996). Therefore, the effect of nickel on steady-state hydrogen transport properties, rather than any transient effect on D_{eff} , has to be considered. At steady state, the hydrogen subsurface concentration at the cathodic

side of the permeation cell, C_0 , is related to the steady-state hydrogen permeation flux, J_{ss} , by Fick's first law:

$$J_{ss} = D_{lat} \cdot \frac{\partial C}{\partial x} = D_{lat} \cdot \frac{C_0}{L}, \quad (9)$$

where D_{lat} is the lattice diffusion coefficient and L is the thickness of the steel sheet. Equation 9 assumes that the hydrogen surface concentration in the anodic side of the Devanathan and Stachurski (1962) experiment is zero. At steady state, hydrogen in the lattice is at equilibrium with hydrogen in traps; in other words, hydrogen absorption rates in traps equal hydrogen desorption. Therefore, the steady-state hydrogen diffusion coefficient approaches the value of the lattice diffusion coefficient (Turnbull & Carroll, 1990), which is larger than D_{eff} (D_{eff} is measured in the rising transient in presence of traps) (Zakroczymski, 1985a). Given that D_{lat} is independent of the chemical composition and microstructure of the alloy for ferritic steels (Turnbull & Carroll, 1990), at steady state, any effect in nickel on C_0 could translate into a measurable change in either K_{i-SSC} or σ_{th-SSC} (Gerberich & Chen, 1975). Rather than calculating C_0 , an alternative is to use the thickness normalized hydrogen diffusion flux, $J_{ss} \cdot L$ (Saenz de Santa Maria & Turnbull, 1989), which can be directly obtained from permeation experiments without any assumption on D_{lat} values. A correlation was found between this quantity and cracking resistance in different environments (Saenz de Santa Maria & Turnbull, 1989).

Although no atomistic HE mechanism has gained the consensus of the community, it is generally accepted that a hydrogen-assisted crack advances only when a critical hydrogen concentration (H_{crit}) is reached ahead of a potential crack site. A potential crack site is a defect in the lattice that acts as a hydrogen trap (Pressouyre, 1980). In this regard, H_{crit} is a function of the applied stress level as well as the type and shape of the trap sites. For example, elongated MnS inclusions have a lower H_{crit} than rounded inclusions and thus have a higher tendency to act as potential crack sites. Other hydrogen traps, like fine carbides, have a higher H_{crit} , retaining hydrogen and slowing down hydrogen transport to sites with lower H_{crit} , where cracks are expected to be nucleated first.

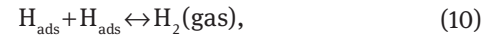
The effects of nickel on hydrogen absorption, trapping, and D_{eff} are discussed in detail in the following sections.

4.2.1 Effect of nickel on hydrogen permeation at steady state

Steady-state permeation as a function of nickel content studies based on the Devanathan and Stachurski cell

(Devanathan & Stachurski, 1962) have given controversial results. Whenever the experimental details reported by the different investigators allowed it, results were presented in a $J_{ss} \cdot L$ vs. nickel content plot (Figure 5). In general, Ni additions resulted in a decrease in $J_{ss} \cdot L$, which, based on Equation 9 and the low variability in D_{lat} values with microstructure and composition for ferritic steels (Turnbull & Carroll, 1990), should be related to a decrease in C_0 with increased Ni content.

Beck, Bockris, Genshaw, and Subramanyan (1971) reported an increase in steady-state hydrogen flux for samples cathodically charged in NaOH when Ni content increased from 0 to 5-wt%. Wilde, Kim, and Turn (1982) systematically studied hydrogen absorption kinetics as a function of noble element additions, including Ni, Cu, Ag, Pd, and Pt, to UNS G41300 (SAE/AISI 4130). Given that noble metals catalyze the recombination of adsorbed atomic hydrogen according to Glasstone (1942),



the authors expected a reduction in hydrogen permeation rates. Wilde et al. (1982) found that, in H_2S -saturated 3.5-wt% NaCl acidified with 0.5-wt% acetic acid, Ni, Pd, and Pt accelerated the rate of the hydrogen evolution reaction (HER), as shown by cathodic polarization curves. However, despite the expected increase in hydrogen recombination rates, the steady-state hydrogen flux increased by about 20% when 1.0-wt% of each of those elements was added to the base alloy, in accord with results by Beck et al. (1971).

Contrary to this finding, Yoshino and Minozaki (1986) found that the surface hydrogen concentration, which is proportional to the steady-state flux, decreased with increasing Ni content in the range of 0–5-wt% for a comparable Cr-Mo-Ni base alloy composition exposed to a similar solution. In contrast, the surface hydrogen concentration remained constant in electrolytes containing no acetic acid. However, Yoshino and Minozaki used D_{eff} values measured in the rising transient to calculate the subsurface hydrogen concentration at steady-state using Equation 9. As D_{eff} decreased with nickel content, and it is always lower than D_{lat} , Equation 9, Yoshino and Minozaki's calculations resulted in a systematic error in the estimation of C_0 . However, by calculating $D_{eff} \cdot C_0$ from reported data by Yoshino and Minozaki, it is possible to obtain the correct of $J_{ss} \cdot L$ value, which is a direct measurement of hydrogen absorption independent of sample thickness. This magnitude decreased with nickel content in both solutions studied by Yoshino and Minozaki (Figure 5), suggesting an inhibiting effect of nickel on SSC intensity.

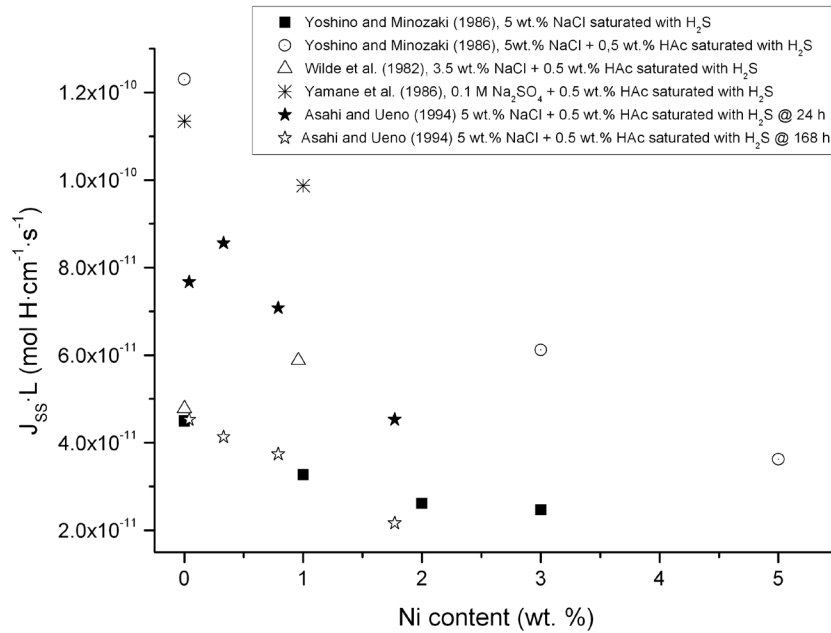


Figure 5 Thickness normalized hydrogen permeation steady-state values as a function of nickel content, obtained by different investigators (Yoshino & Minozaki, 1986; Wilde et al., 1982; Yamane et al., 1986; Asahi & Ueno, 1994) using the Devanathan and Stachurski technique (Devanathan and Stachurski, 1962).

Steels had, in addition to nickel as indicated, 0.2-wt% C, 0.25-wt% Si, 0.6-wt% Mn, 1-wt% Cr, 0.5-wt% Mo, 0.02-wt% Al, 0.006-wt% S, and 0.01-wt% P for steels used by Yoshino and Minozaki (1986), 0.37-wt% C, 0.29-wt% Si, 0.6-wt% Mn, 0.19-wt% Mo, 1.1-wt% Cr, 0.014-wt% S, and 0.006-wt% P for steels used by Wilde et al. (1982), 0.12-wt% C, 0.25-wt% Si, 1.02-wt% Mn, 0.05-wt% Mo, 0.02-wt% V, 0.001-wt% B, 0.003-wt% S, and 0.003-wt% P for steels used by Yamane et al. (1986), and 0.2-wt% C, 0.05-wt% Si, 0.5-wt% Mn, 0.2-wt% Mo, 0.03-wt% Nb, 0.02-wt% Al, 0.01-wt% Ti, 0.008-wt% P, 0.001-wt% S, 0.0025-wt% N, and 0.001-wt% B, for steels used by Asahi and Ueno (1994), with permission of © NACE International, 1982, 1986.

In accord with results by Yoshino and Minozaki (1986), Yamane et al. (1986) reported a decrease in steady-state hydrogen permeation values in the entire -0.6 to +0.2 V vs. E_{oc} potential range for a LAS containing 1-wt% Ni exposed to a 0.1-M Na₂SO₄ solution saturated with either 3000 ppm H₂S or 100 ppm H₂S. This decrease in permeation current with nickel content was in accord with a slight increase in failure time at constant load and under applied cathodic potentials, where the effect of Ni on localized corrosion (e.g., trenching, Section 4.3) can be ignored (Figure 6). Similarly, for hydrogen permeation tests performed in 2-mm-thick steel membranes with varying nickel content in the 0- to 1.7-wt% range, Asahi and Ueno (1994) showed that at steady state, i.e., after 168 h, hydrogen permeation decreased with an increase in Ni content. These results correlated with a slightly higher $K_{I,SSC}$ in samples with increased Ni content (Asahi & Ueno, 1994). Interestingly, $J_{ss} \cdot L$ was lower at 168 h than at 24 h (Figure 5). These examples illustrate that, due to the formation and thickening of sulfide films that hinder hydrogen permeation, long-term experiments are necessary to obtain an actual steady-state hydrogen permeation value (Asahi et al., 1994; Kappes et al., 2012; Tsai & Shih, 1998).

Other authors used the hydrogen desorption technique to study the amount of diffusible hydrogen as a function of nickel content. The hydrogen desorption technique consists on charging a steel sample by immersion in the environment of interest for a given time. Subsequently, cleaning of the surface is usually done by polishing to remove corrosion products that might hinder hydrogen desorption. The sample is finally left immersed in mercury or other inert fluid where hydrogen is desorbed and the volume measured with a eudiometer. Yoshino (1982) determined that the absorbed hydrogen in H₂S-saturated 5-wt% NaCl solution acidified with 0.5-wt% acetic acid was in the 4-ppm range and independent of Ni content in bainitic LAS. Quenched and tempered, either in cast or forged condition, Cr-Mo-Ni-steels with Ni contents close to 2.7-wt% absorbed less hydrogen than Cr-Mo steels with Ni below the 1-wt% threshold (Webster, Austen, & Rudd, 1985). Gooch (1982a, b), studying LAS-welded samples with 2-wt% Ni exposed to the same NaCl-acetic acid solution used by Yoshino found that in the first 100 h, hydrogen absorption was higher in the nickel-containing samples than in the Ni-free control samples. However, measurements at 525 h, where a steady state was probably

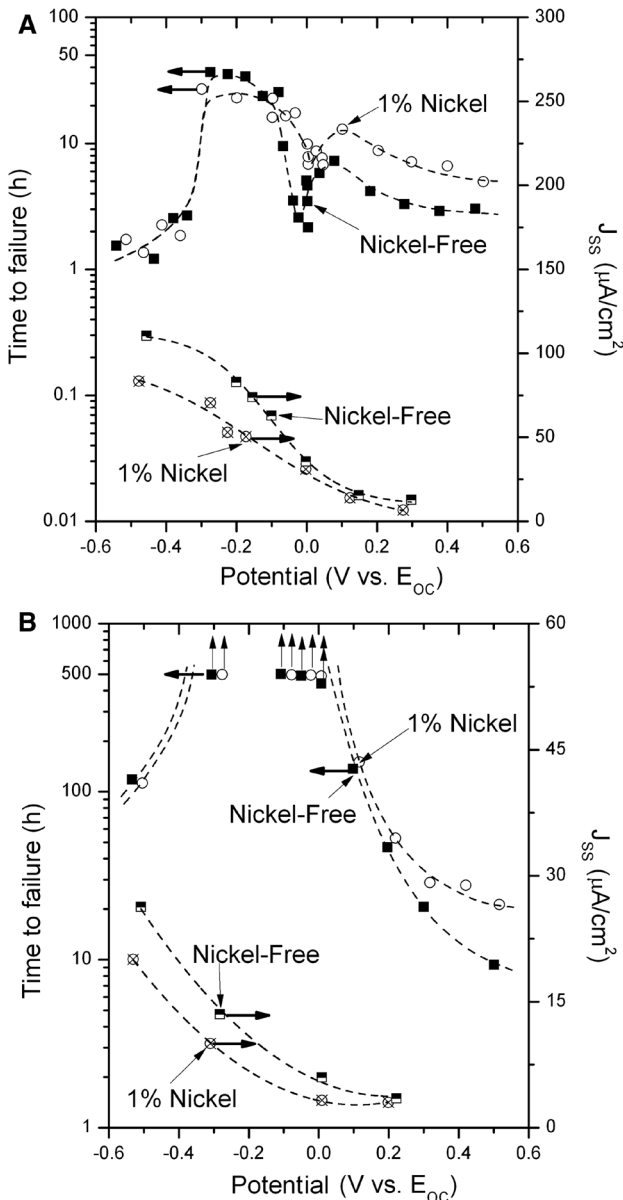


Figure 6 Time to failure of specimens with a constant load equivalent to 80% YS and steady-state hydrogen permeation (J_{ss}) as a function of potential in a solution of 0.1 M Na_2SO_4 acidified with 0.5-wt% acetic acid, saturated with (A) H_2S and (B) 100 ppm H_2S (Yamane et al., 1986).

Dashed lines were added as a guide for visualization, © NACE International, 1986.

reached, revealed that the hydrogen content of nickel-containing samples was lower than that of the control. Furthermore, the hydrogen content in the nickel-containing weld metal was always lower than in the base metal, which had 0.02-wt% Ni.

It is interesting that the hydrogen content in the 2-wt% nickel-containing sample was higher at 100-h than at 525-h (Gooch, 1982a, b), in contrast to the control sample,

where hydrogen content increased with increasing exposure time. This could be related to the well-documented decrease in hydrogen absorption rates caused by the formation of iron sulfide films (Asahi et al., 1994; Kappes et al., 2012; Tsai & Shih, 1998). There are few experiments where hydrogen permeation was studied for such long times in nickel-containing samples. However, results by Tsai and Shih (1998) for a LAS containing 0.2-wt% Ni exposed to H_2S -saturated 5-wt% NaCl solution acidified with 0.5-wt% acetic acid showed that hydrogen permeation peaks after few hours and then starts to decrease. This is believed to be due to the formation of iron sulfide films, which decreases both the hydrogen concentration at the surface and the uniform corrosion rate of the alloy. Tsai and Shih (1998) acknowledged the possibility that, after reaching the hydrogen permeation peak, diffusible and reversibly trapped hydrogen could desorb from the metal due to the concentration gradient between the surface and the bulk. A mechanism based on sulfide film formation could explain the lower hydrogen content in the sample exposed for 525-h shown by Gooch. In accord to this, Asahi and Ueno (1994) showed that increasing nickel content resulted on a faster decrease on steady-state hydrogen permeation with time than on Ni-free control samples. However, a better understanding regarding the structure and composition of the sulfide film formed as a function of nickel content in LAS is needed to explain why this reversal was not observed in the control sample (Gooch, 1982a,b).

4.2.2 Effect of nickel on effective hydrogen diffusion coefficient

Beck et al. (1971) studied the effect of nickel on hydrogen diffusion in Fe-Ni alloys with Ni varying from 0-% to 100-wt% and exposed to a cathodic current with no H_2S additions. Alloys were annealed at a non-specified temperature and then slowly cooled to room temperature. Assuming the heat treatment was such that equilibrium was reached, the alloys likely consisted of α phase for pure iron and Fe-5-wt% Ni, $\alpha+\gamma$ phases for alloys with Ni content between 10- and 40-wt%, and γ phase for Fe-Ni alloys with % Ni >60-wt%. For the Fe-5-wt% Ni alloy, the authors found that the D_{eff} was lower than for pure iron (Beck et al., 1971). Further nickel additions caused a step decrease in hydrogen diffusion coefficient, which was interpreted in terms of the dual-phase nature of the alloy. An increase in the nickel concentration beyond 8-wt% increases the volume fraction of austenite, reducing hydrogen diffusivity. In this regard, while hydrogen solubility is

significantly higher in austenite than in ferrite, hydrogen diffusivity is slower in an fcc structure than in a bcc lattice as previously noted.

Other authors concentrated their studies on alloys with lower nickel contents, in the range of interest of LAS. Yoshino and Minozaki (1986) studied hydrogen permeation in 0.2-wt% C Cr-Mo-Ni-steels exposed to H₂S-saturated 5-wt% NaCl with and without addition of 0.5-wt% acetic acid at E_{oc}. In both cases, the hydrogen diffusion coefficient decreased with an increase in nickel content in the 0- to 5-wt% range, in accord with results by Beck et al. (1971). Wilde et al. (1982) also reported a decrease in the hydrogen diffusion coefficient when 1-wt% Ni was added to a UNS G41300 (SAE/AISI 4130) alloy exposed to a H₂S-saturated 3.5-wt% NaCl solution acidified with 0.5-wt% acetic acid.

4.2.3 Effect of nickel on hydrogen trapping

Given that nickel does not form carbides, the effect of nickel on hydrogen trapping can be divided into (i) direct effects, due to the presence of Ni in solid solution in the ferrite phase, or (ii) indirect effects, due to the effect of nickel in refining microstructure.

Similar to other substitutional atoms like Mn, Cr, V, Nb, and Ti, Ni behaves as a reversible hydrogen trap (Pressouyre, 1979). Reversible traps can act as sources or sinks of hydrogen, depending on the type of test (Pressouyre, 1980). The interaction energy between hydrogen and Ni is lower than that of common substitutional elements found in steels (Pressouyre, 1979). Therefore, nickel acts as an extremely weak hydrogen trap, resulting in a smaller decrease in D_{eff} than when the same amount of Cr or Ti is added to the steel (Pressouyre & Bernstein, 1978). Beck et al. (1971) found a 20% decrease in the D_{eff} with a 5-wt% nickel addition, which is well below the tenfold decrease in D_{eff} for a 1.5-wt% Ti addition reported by Pressouyre and Bernstein (1978).

The beneficial effect of decreased grain size on hydrogen-assisted cracking resistance of LAS is well established (Bernstein & Thompson, 1976). Given that nickel decreases the A_{cl} temperature of the steel and refines microstructure, nickel additions to LAS are expected to increase HE resistance (Chavane, Habashi, Pressouyre, & Galland, 1986). The grain boundary area per unit volume and the number of carbides per unit volume both increase when the microstructure, i.e., both grain and carbide size, are refined. In this regard, high-angle grain boundaries and carbide interphases are considered irreversible traps (Pressouyre, 1980). Although carbides can act as potential

flaws (Yoshino, 1983), this effect is minimized when they are finely distributed in the microstructure. Finely distributed carbides, being irreversible traps, act as sinks of hydrogen and therefore slow down hydrogen transport to the crack tip. As a result, nickel is expected to increase SSC resistance (Pressouyre, 1979). In contrast, other irreversible traps, such as MnS and oxide interphases, are undesirable because they can act as potential flaws themselves (Chavane et al., 1986). Stringent maximum sulfur content limits and strict control of shape and distribution of inclusions is paramount for maximum SSC resistance (EFC, 2009; Kimura et al., 1989; NACE-ISO, 2001), e.g., API 6A Table 10 and API 5CT Tables C.5 (API, 2004, 2010).

4.3 Effect of Ni on pitting/trenching

Several investigators have reported surface damage in the form of pits, trenches, and/or small blunt cracks when Ni-containing LAS were exposed to sour environments (Dunlop, 1978; Kaneko & Ikeda, 1988; Yamane et al., 1986; Yoshino & Minozaki, 1986). It is implicit in the papers that the depth-to-diameter ratio increases in the order those features were mentioned above; however, limits in aspect ratio to distinguish between them were not established. Furthermore, the use of terms like “sharp pits” or “micro-cracks” makes the distinction between them even fuzzier. Payer et al. (1986) also observed those surface defects, not only in Ni containing but also in Ni-free LAS. Payer et al. observed that the trenches were present on specimens stressed near $\sigma_{th,SSC}$ and that the depth was a function of applied stress, similar to what was presented by Yoshino and Minozaki (1986). Nevertheless, it was also proposed that Ni is not a prerequisite for their presence (Craig, 1988; Payer et al., 1986), as they were observed in stressed steels with no nickel (Colwell, Payer, & Boyd, 1986) or in steels with nickel content well below the 1% threshold (Ikeda, Kaneko, & Ando, 1987; Kaneko & Ikeda, 1988; Wilde & Doyle, 1979).

In a later investigation, Craig et al. (1990) observed that increased Ni contents appeared to promote deeper, “crack-like” trenches (Figure 7). Yamane et al. (1986) also reported an increase in trench aspect ratio with increasing Ni content in the 0.5- and 2-wt% Ni range and at a dissolved H₂S concentration of 100-ppm. The density, depth, and trench aspect ratio shown by Yamane et al. leveled out at 1-wt% Ni. This independence of trench aspect ratio for a nickel content beyond 1-wt% also challenges ISO 15156-2 limitation on nickel content (NACE-ISO, 2001).

There is consensus between different authors that trench formation and morphology is a function not only of

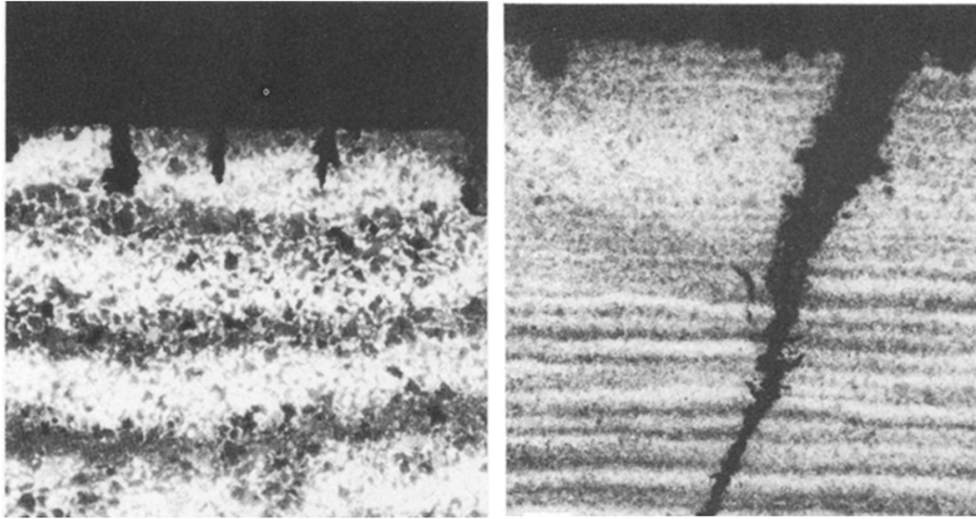


Figure 7 Cross sections of smooth tension specimens, showing surface attack in a solution containing 5-wt% NaCl and 0.5-wt% acetic acid and saturated with H_2S .

Specimens loaded to 80% YS. (A) 2% Ni and (B) 4% Ni. Normalized specimens, magnification 100 \times (original magnification), Nital etch. After Craig (Craig et al., 1990), © NACE International, 1990.

alloy composition but also stress level, hardness, and solution composition (Colwell et al., 1986; Craig et al., 1990; Yamane et al., 1986). Trench formation seems to be related to both low- and high-strength steels exposed to H_2S partial pressures, p_{H_2S} , close to the σ_{th-SSC} (Colwell et al., 1986). Higher P_{H_2S} promoted SSC, which is characterized by sharp propagating cracks with aspect ratios >100–500:1 (Colwell et al., 1986; Craig, 1988; Pargeter, 2000). In certain cases, a trench can act as an initiation point for a sulfide stress crack, if K_{I-SSC} is exceeded.

As discussed by Craig (1988) and Yoshino and Minozaki (1986), tests conducted in solutions without NaCl, e.g., NACE TM0177 Method B, have a tendency to enhance trenching. This test is more sensitive to crack initiation than crack propagation (Yoshino & Minozaki, 1986); therefore, any possible negative effect of nickel on trenching and crack initiation might be exacerbated. For example, after performing tests in a solution without sodium chloride, Yamane et al. (1986) reported a correlation between Ni content and both trench density and aspect ratio.

Yoshino and Minozaki (1986) presented anodic and cathodic polarization curves of steels with varying nickel content in 5-wt% NaCl solution saturated with H_2S . E_{oc} increased from -668 to -625-mV vs. SCE when the nickel content increased from 0 to 3-wt%. Likewise, the corrosion current density (i_{corr}) as inferred by the Tafel extrapolation method, increased with nickel from approximately 44 $\mu A/cm^2$ for 0-wt% Ni to about 75 $\mu A/cm^2$ for 3-wt% nickel, which can be explained by the increase in the cathodic reaction rate as a function of nickel. This increase in

cathodic reaction and E_{oc} corrosion rate is in marked contrast with the decrease in hydrogen permeation at steady state for the same alloys in the same environment (Figure 5). Interestingly, at an arbitrary anodic polarization potential of -500-mV vs. SCE nickel decreased the kinetics of the anodic reaction. Similar results were presented by Wilde et al. (1982) in 5-wt% NaCl solution acidified with 0.5-wt% acetic acid and saturated with H_2S . Yoshino and Minozaki (1986) suggested that a protective film provided generalized corrosion protection but could promote trenching. Considering this, the difference in trenching susceptibility between tests with and without NaCl could be related to differences in the stability of such film. Likewise, this film could also explain the decreased hydrogen absorption rate. However, other than what can be indirectly inferred from polarization curves, no evidence of the existence of such film has been presented to date. Moreover, the formation of a protective film is difficult to justify based on the shape of the anodic polarization curves obtained by Yoshino and Minozaki (1986). In this regard, anodic Tafel slopes were in the 107- to 117-mV/decade-1 range, which is within the range expected for activation polarization without rate-limiting film formation.

4.4 Effects of plastic deformation

In more recent investigations, Craig et al. (1990) Craig, Brownlee, and Bruno (1992) studied the effects of nickel, from 0- to 8-wt%, on SSC of LAS. The authors found that

the difference between the proportional limit and the 0.2% offset YS in LAS increases with an increase in nickel content, up to 40% for Ni contents higher than 3-wt%. Therefore, when tests were conducted at a fixed fraction of the 0.2% offset YS in an attempt to compare the effect of Ni on SSC resistance, Ni-containing LAS ended up being stressed above their proportional limit and underwent more plastic deformation than Ni-free steels. When normalized to their proportional limit, LAS having <2-wt% Ni failed by SSC under elastic strain, and those LAS with higher nickel contents failed under plastic deformation. When the effect of nickel on the proportional limit is taken into account, the authors concluded that Ni-steels having more than 2-wt% Ni had a better SSC performance than those with lower Ni contents, (Craig et al., 1992). For steels with Ni content below 2-wt%, the proportional limit and 0.2% offset YS differ in <10% (Craig et al., 1992), and they have SSC resistance equivalent to Ni-free steels when properly heat treated (Craig et al., 1990).

Because plastic deformation favors hydrogen absorption (Huang, Nakajima, Nishikata, & Tsuru, 2003; Snape, 1967), this could explain the negative effect on SSC performance attributed to nickel (Craig et al., 1992). There are two major physical interactions between hydrogen and plastic deformation that could explain this increased hydrogen absorption, i.e., enhanced transport by moving dislocations and enhanced trapping of hydrogen due to increased dislocation density (Huang et al., 2003; Zakroczymski, 1985).

Other authors also concluded that Ni-containing steels underperformed Ni-free steels in tests that involved plastic deformation (Kaneko & Ikeda, 1988; Treseder & Swanson, 1968). Those tests include NACE TM0177 Method B bent-beam test (NACE, 1996), and SSRT. Trenches and cracks were reported near the stress raisers of the bent-beam test by Treseder and Swanson (1968) and Dunlop (1978) in steels with Ni contents above 1-wt%. Kaneko and Ikeda (1988) reported increased tendency to trench formation in this test even in samples with 0.48-wt% Ni. As mentioned before, the presence of the stress raisers in the bent-beam results in local plastic deformation (Snape, 1968a).

Although it seems plausible to assume that plastic deformation and trenching are related processes, conflicting results have been reported in SSRT of Ni-containing steels in sulfide environments. Kaneko and Ikeda (1988), using a strain rate of 10^{-6} s^{-1} , reported that the ductility loss with up to 0.48-wt% Ni was similar than for the Ni-free control samples. Increased tendency for trenching was observed even at this low Ni contents in the NACE TM0177 Method B bent-beam tests (Kaneko & Ikeda, 1988). The authors concluded that, given the relatively fast strain rate

used in the SSRT, there was insufficient time for trenches to develop; however, the authors did not prove this argument by conducting tests at a lower strain rate level. No trenches were observed by Yoshino and Minozaki (1986) for Ni contents up to 4-wt% in SSRT performed in H_2S -saturated 5-wt% NaCl solution at strain rates down to $3 \times 10^{-6} \text{ s}^{-1}$. In fact, the authors observed that elongation to failure slightly increased with nickel content, especially at faster strain rates, probably due to the decrease in hydrogen diffusivity with Ni content (Yoshino & Minozaki, 1986). Therefore, if trenching is minimized, Ni-containing LAS under plastic deformation are not more susceptible than Ni-free steels.

Erlings, De Groot, and Nauta (1987) reported failures at stress levels just above the YS for steels with 3.5-wt% Ni in H_2S -saturated 5-wt% NaCl solution acidified with 0.5-wt% acetic acid tested at strain rates $2 \times 10^{-7} \text{ s}^{-1}$ and slower (i.e., almost an order of magnitude slower than Yoshino and Minozaki). Failures were accompanied by trenching and anodic dissolution. However, when the same steel was pre-stressed in air to the UTS and then loaded by the SSRT in the environment in the elastic region, the specimen did not fail, suggesting that plastic deformation concomitant with exposure to the environment is required for failure to occur (Erlings et al., 1987). In addition, trenches and pits were observed in smooth specimens that were stressed at a constant load below the YS, but no cracks developed at the bottom of those specimens. Under conditions leading to trenching and with some degree of plastic deformation applied, such defects could act as strain concentrators aiding in the crack nucleation process.

4.5 SSC propagation mechanisms of LAS

Tests at different potentials are useful for establishing plausible crack propagation mechanisms (Latanision, Gastine, & Compeau, 1977). In this regard, given the increase overpotential for the HER, hydrogen-assisted mechanisms are exacerbated by applied cathodic potentials but suppressed at anodic potentials above the reversible H/H^+ potential, $E_{\text{H}/\text{H}^+}^{\text{Rev}}$. In contrast, cracking modes that rely on the formation and cracking of pseudo-protective surface films or on active path corrosion (APC) are typically aggravated by applied anodic potentials and inhibited at potentials below E_{oc} (Wilde, 1971). However, it has been demonstrated that hydrogen can be absorbed even under an anodic polarization (Barth, Steigerwald, & Troiano, 1969), as long as the potential is kept below $E_{\text{H}/\text{H}^+}^{\text{Rev}}$. Hydrogen absorbed at anodic potentials can assist the crack propagation process. This case is usually found

in passivated or film-covered metals under localized corrosion (Barth et al., 1969; Wilde, 1971). Under this scenario, acidified conditions at the localized corrosion site can enhance hydrogen absorption (Wilde, 1971).

Dunlop (1978), after conducting tests at E_{oc} and a cathodic potential, was the first to suggest that cracking of nickel-containing LAS in H_2S environments could be rate controlled by an anodic mechanism, rather than by the commonly accepted hydrogen-assisted model for LAS (Berkowitz & Heubaum, 1984; Snape, 1967; Turn et al., 1983). The author exposed NACE TM0177 Method B bent-beam specimens containing 3.5-wt% Ni normalized to hardness well below the 22-HRC threshold to a 0.5-wt% acetic acid solution saturated with H_2S or H_2S+N_2 gas mixtures. The most interesting finding was that a cathodic polarization decreased, rather than enhanced, the amount of crack growth, as it would be expected based on the correlation between hydrogen permeation and SSC intensity with cathodic potentials (Berkowitz & Heubaum, 1984). Therefore, Dunlop concluded that crack growth was controlled by an anodic mechanism.

Dunlop's work was later criticized by Uhlig (1978) and Craig (1982). Uhlig suggested that, as a result of the cathodic polarization imposed on the electrode, the pH might have increased significantly up to the point where HS^- rather than H_2S predominated in the surface. This, according to Uhlig, could negatively affect hydrogen absorption rate because HS^- is not as effective as H_2S in poisoning the hydrogen recombination reaction. In response, Dunlop (Uhlig, 1978) estimated, neglecting the influence of acetic acid to give a conservative upper limit, a pH change within 2 pH units, increasing from 4 to 6 at the electrode surface. Craig suggested that the amount of HS^- abruptly increased in this pH region at the expense of H_2S , citing a H_2S speciation diagram (Hudgins et al., 1966). However, this diagram shows that even at pH 6, the H_2S/HS^- ratio should be >10 . Furthermore, something that is missing in the discussion by Uhlig and Craig is that the hydrogen absorption rate is not controlled by the concentration of hydrogen recombination poisons alone, but also by the rate of hydrogen evolution, which effectively increases with a cathodic overpotential. Later work by Berkowitz and colleagues (Berkowitz & Heubaum, 1984; Berkowitz & Horowitz, 1982) in a 5-wt% NaCl solution acidified with 0.5-wt% acetic acid and saturated with H_2S revealed that both hydrogen evolution and absorption rates, measured with the Devanathan and Stachurski cell (Devanathan & Stachurski, 1962), monotonically increased as a function of cathodic overpotential. Therefore, neglecting the secondary effects caused by the addition of 5-wt% of NaCl, it can be concluded that in the tests conducted by Dunlop

the hydrogen absorption rate did, in fact, increase with a cathodic potential (Dunlop, 1978).

As discussed above, it is likely that hydrogen absorption increased with the HER overpotential in the tests conducted by Dunlop (1978). Therefore, the anomalous effect of potential on cracking reported by Dunlop in sulfide-containing environments could be related to the presence of pits and trenches, which were reported by the author on NACE TM0177 Method B bent-beam specimens (Dunlop, 1978). Given that pits and trenches are the result of anodic dissolution, they are favored at anodic rather than cathodic overpotentials. Against current NACE TM0177 recommendations (NACE, 1996), which suggest to clean the specimens mechanically to remove corrosion products or to conduct cross-section analysis, Dunlop bent the specimens after removing them from the environment to evaluate the presence of cracks. Thus, it cannot be stated whether the cracks grew in the environment or after removal from the environment during the bending step, where pits and trenches could act as stress raisers, as criticized by Craig (1982). Considering the effect of potential on pit and trench formation, this explanation would explain the lower cracking rate with a cathodic potential. Thus, it is possible to assume that the samples exposed to a cathodic potential exhibited less cracking due to the reduced amount of stress concentrators active during the post-test bending step.

All steels used by Dunlop in his investigation had a fixed nickel concentration close to 3.5-wt%. Therefore, beyond all criticism to the test methodology exposed here, no conclusions on the effect of nickel could be drawn. Schmid (1980) conducted constant load SSC tests on the same 3.5-wt% Ni ASTM A203 grade E steel. Given that the author did not specify heat treatment and microstructure, limited information can be obtained from that paper. However, Schmid concluded that this alloy had a higher σ_{th-SSC} than a 1-wt% Ni LAS of similar hardness, concluding that Ni had no adverse effect on SSC performance.

Localized dissolution, in the form of pits and trenches, is associated with the presence of surface films. Formation of a non-stoichiometric $Fe_{(1+x)}S$ film, where the x can take on values between 0 and 0.11 (Shoosmith, Taylor, Bailey, & Owen, 1980; Smith & Miller, 1975), can provide some degree of general corrosion protection, which is evidenced by a decrease in generalized corrosion measured with weight-loss coupons and hydrogen permeation rates with time (Azevedo, Bezerra, Esteves, Joia, & Mattos, 1999). If $Fe_{(1+x)}S$ films were more protective in Ni-containing steels, that would explain the reduced amount of hydrogen permeation at steady state (Asahi & Ueno, 1994; Yamane et al., 1986; Yoshino & Minozaki, 1986) and the increased amount

of trenching in the alloys reported by some authors (Craig et al., 1990; Yamane et al., 1986). This is a purely speculative assumption that should be validated with long-term corrosion tests. Furthermore, potentiostatic tests held at a net cathodic potential to yield a similar rate of hydrogen permeation in H_2S -free environments, but with the addition of H recombination poisons (Berkowitz & Heubaum, 1984), could help to weigh the relative importance of hydrogen absorption vs. anodic dissolution based mechanisms on cracking of nickel-containing steels.

Yoshino and Minozaki (1986) investigated cracking of Ni LAS under both anodic and cathodic polarizations. The authors conducted galvanostatic SSRT of a laboratory melt steel containing 5-wt% Ni and a nickel-free control sample with a base composition of 0.2-wt% C, 0.6-wt% Mn, 1-wt% Cr, and 0.5-wt% Mo. In clear contrast to the work by Dunlop (1978), Yoshino and Minozaki showed that elongation to failure increased with an anodic potential and decreased with a cathodic potential (Figure 8), suggesting that cracking was assisted by hydrogen for both materials at E_{oc} . Hydrogen permeation measurements confirmed an increase in the hydrogen absorption rate with an applied cathodic overpotential (Figure 8), explaining the decrease in ductility based on increased hydrogen absorption. The authors observed some trenches in the sample exposed at OCP, which suggests competition between an anodic dissolution based mechanism and HE. However, the shape of the elongation to fracture vs. potential curve clearly suggested hydrogen effects were prevalent (Figure 8). At an anodic overpotential, the elongation to fracture was well below the air-measured value. Pits and trenches were observed under anodic polarization, and they likely contributed to the decrease in mechanical properties. At sufficiently high anodic overpotential, the hydrogen absorption rate started to increase again (Figure 8), which could be related to hydrogen absorption at pit bottoms (Yoshino & Minozaki, 1986). At this point, a transition from active dissolution to HE could occur. This possibility was also postulated by other authors (Yamane et al., 1986).

Yamane et al. (1986) also studied the effect of potential in cracking susceptibility in 0.1-M Na_2SO_4 solutions acidified with 0.5-wt% acetic acid saturated with H_2S (the dissolved H_2S concentration was about 3000-ppm) and at a dissolved H_2S concentration of 100-ppm. This author obtained different results for the effect of potential on SSC intensity (Figure 6). One thing to bear in mind when comparing those results with the ones obtained by Yoshino and Minozaki (1986) is that the SSC intensity was studied under constant load by exposing Ni-free samples and samples containing 1-wt% Ni at 80% YS. In a constant load test, time to failure is the sum of crack

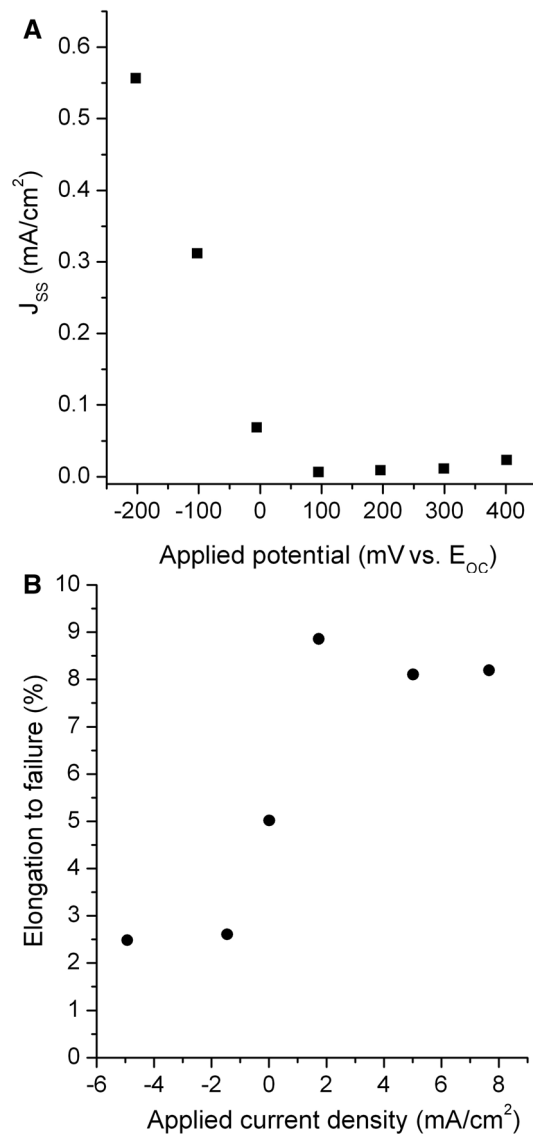


Figure 8 (A) Permeation current as a function of polarization potential and (B) elongation to failure of a 5-wt% Ni steel measured in an SSRT as a function of applied current density.

Tests performed in a solution containing 5-wt% NaCl, acidified with 0.5-wt% acetic acid, and saturated with H_2S (Yoshino & Minozaki, 1986), © NACE International, 1986.

initiation and crack propagation time, whereas in an SSRT test, the elongation to fracture is more sensitive to crack growth. For both H_2S concentrations, time to failure had a similar dependence on potential, regardless of Ni content. This suggests that a similar mechanism controls SSC of Ni-containing and Ni-free LAS. In tests conducted by Yamane et al. (1986), an anodic potential decreased the time to failure for both concentrations, and a negative effect of nickel can be observed (Figure 6). Meanwhile, a cathodic potential initially caused an increase in time to failure, but at sufficiently negative potentials, time to

failure decreased with increasing overpotential, suggesting that in this region cracking was controlled by a HE mechanism. The maximum in time to failure at potentials slightly cathodic with respect to E_{OC} could be related to the decreased effect of trenching on crack initiation. Time to failure of Ni LAS was slightly larger than that of Ni-free steels in the cathodic region, in accord with the decrease in steady-state hydrogen permeation in Ni-containing LAS (Yamane et al., 1986). A minimum in time to failure was observed for samples exposed to 3000-ppm H_2S at E_{OC} , possibly due to cooperation between active dissolution and HE mechanisms. The authors suggested that, in this case, crack growth was controlled by a mechanism where cracks initiated by anodic dissolution and then grew by a HE-based mechanism once the crack reached a critical depth, as previously proposed by Okada, Yukawa, and Tamura (1976) (Figure 9). Notice that at E_{OC} , time to failure is longer for Ni-containing than for Ni-free steels.

For lower H_2S concentrations in the 100-ppm range, crack growth was accelerated by an anodic potential and a negative effect of nickel was evident in the region of high anodic overpotential (Figure 6). Whereas an increase in cathodic overpotential below -0.3-V vs. E_{OC} resulted in no failure, at potentials more negative than this, time to failure decreased with an increase in cathodic overpotential. Yamane et al. (1986) and Motoda, Yamane,

Uesugi and Nakai (1981) concluded that crack propagation at E_{OC} was controlled by anodic dissolution for low H_2S concentrations. However, it is well known that hydrogen can be absorbed even under an anodic polarization below E_{H/H^+}^{Rev} , and the fact that time to failure decreases with anodic overpotential cannot be used to rule out a hydrogen-based mechanism (Barth et al., 1969). Hydrogen permeation experiments by Yamane et al. were studied up to 0.2-V vs. E_{OC} , and no increase in hydrogen permeation was apparent (Figure 6). However, Yoshino and Minozaki (1986) showed that at overpotentials above 0.4-V vs. E_{OC} , the hydrogen permeation started to increase, which was related to increased hydrogen evolution at pit bottoms (Figure 8). Despite the fact that the hydrogen permeation current under an anodic overpotential was lower than that obtained at a cathodic overpotential, it has to be normalized by a smaller area giving a large local hydrogen absorption density. Moreover, considering that this hydrogen is absorbed directly at the bottom of a stress concentration point, the diffusion distance is decreased and it is expected to directly enhance crack propagation kinetics.

Based on what was exposed in this section, it is concluded that “elongated” pits or trenches could have a significant role in SSC at E_{OC} by acting as stress concentrators (Ikeda et al., 1987) or as initiation sites for SSC (Yamane et al., 1986). Crack growth in Ni alloy steels seems to be controlled by an HE process, which is no different than that of Ni-free LAS. Tests with pre-cracked specimens sensitive to either crack growth or to the SSC arrest stress intensity factor (Asahi & Ueno, 1994; Craig, 1988; Motoda and Yamane, 1981; Yamane et al., 1986) or SSRT at insufficiently low strain rates (Kaneko & Ikeda, 1988), where there is not enough time for trenches to develop due to the short duration of the exposure, are insensitive to the effect on Ni on trenching, which merely acts on the crack initiation stage.

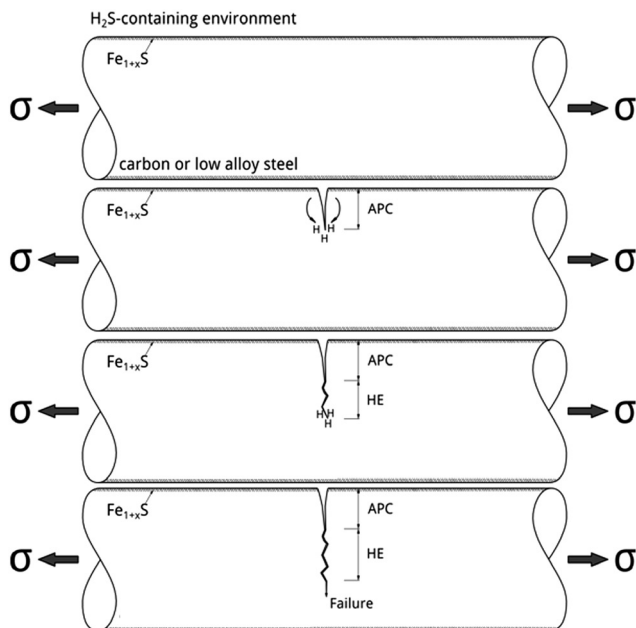


Figure 9 SSC initiation and propagation mechanism for nickel alloy steels (Yamane et al., 1986), involving transition from APC to HE. Tensile stress, σ , could be externally applied or a result of residual stresses, © NACE International, 1986.

5 Conclusions

This review discussed the effect of nickel additions to LASs on phase transformation kinetics, mechanical properties, and SSC resistance. The following conclusions were drawn based on the evidence presented herein:

1. Nickel additions to LASs improve strength, low-temperature fracture toughness, and hardenability with limited impact on CE. No other alloying element improves strength and toughness simultaneously without a significant effect on weldability.
2. In combination with Cr and Mo, Ni is perhaps the most important alloying element to obtain homogeneous

properties through-thickness and/or DBTT below -60°C , which cannot be achieved by refining grain size alone.

3. Although research has shown that nickel has no direct deleterious effect on SSC resistance, crack initiation and propagation mechanisms in both nickel-containing and nickel-free LAS are still unclear. Whereas crack initiation at E_{oc} seems to be controlled by the competition between localized corrosion and hydrogen absorption, crack propagation appears controlled by hydrogen transport exclusively.
4. Regardless of the actual cracking mechanisms, SSC resistance is related primarily to the alloy's microstructure. In this regard, fully tempered martensite showed the best sour service performance, followed by lower bainite. In contrast, untempered martensite and upper bainite reduce SSC resistance significantly and shall be avoided.
5. ISO 15156 1-wt% Ni maximum limit remains greatly controversial and excludes a significant number of high-strength and high-toughness LAS from sour service applications, mandating complicated and expensive qualification testing. In practice, limiting nickel content to 1-wt% constraints materials selection and imposes serious economic and operational penalties for both HPHT and/or arctic O&G operations.
6. Despite the effort to date, more research is necessary to separate the effect of Ni from that of other variables such as alloy composition, microstructure, and loading conditions.
7. Elucidating if LAS with nickel contents above the current 1-wt% limit are fit for sour service will be a technology enabler for the development of the O&G reservoirs of the future.

Acknowledgments: We thank Atle H. Qvale, Bruce Craig, Jan Ivar Skar, Stein Olsen, Roy Johnsen, Alexander Fjeldy, and Anders Wiktorsson for their guidance, support, and technical discussions. This work was sponsored in part by General Electric (Oil and Gas, Norway), The University of Akron (Akron, OH), and the Instituto de Tecnología Profesor Jorge Sabato, Comisión Nacional de Energía Atómica, Centro Atómico Constituyentes (San Martín, Buenos Aires, Argentina).

References

Andrews K. Empirical formulae for the calculation of some transformation temperatures. *JISI* 1965; 203: 721–727.

- ANSI-NACE. Materials resistant to sulfide stress cracking in corrosive petroleum refining environments. ANSI/NACE standard MR0103-2012. Houston, TX, USA: NACE International, 2012.
- API. Specification for casing and tubing. API 5CT (ISO 11960:2001). Washington, DC: API, 2004.
- API. Petroleum and natural gas industries – steel pipe for pipeline transportation systems. API 5L (ISO 3183:2007). Washington, DC: API, 2007.
- API. Specification for wellhead and Christmas tree equipment. API 6A. Washington, DC: API, 2010.
- API. High-pressure high-temperature (HPHT) design guidelines, 1st ed. (draft). API technical report 17TR8. Washington, DC: API, 2013.
- Asahi H, Ueno M. Effects of Ni addition on sulfide stress cracking resistance of low alloy tempered martensite steels. *ISIJ Int* 1994; 34: 290–294.
- Asahi H, Sogo Y, Ueno M, Higashiyama H. Metallurgical factors controlling SSC resistance of high-strength, low-alloy steels. *Corrosion* (Houston, TX, USA) 1989; 45: 519–527.
- Asahi H, Ueno M, Yonezawa T. Prediction of sulfide stress cracking. *Corrosion* (Houston, TX, USA) 1994; 50: 537–545.
- ASTM. Standard specification for alloy-steel and stainless steel bolting for low-temperature. ASTM A320/320M. West Conshohocken, PA: ASTM International, 2010a.
- ASTM. Standard specification for pressure vessel plates, five percent nickel alloy steel, specially heat treated. ASTM standard A645/A645M-2010. West Conshohocken, PA: ASTM International, 2010b.
- ASTM. Specification for pressure vessel plates, alloy steel, double-normalized and tempered 9% nickel. ASTM standard A353/A353M-2009. West Conshohocken, PA: ASTM International, 2014.
- AWS. Structural welding code – steel. AWS D1.1/D1.1M. Miami, FL: AWS, 2002.
- Azevedo C, Bezerra PSA, Esteves F, Joia CJB, Mattos OR. Hydrogen permeation studied by electrochemical techniques. *Electrochim Acta* 1999; 44: 4431–4442.
- Barth C, Steigerwald E, Troiano A. Hydrogen permeability and delayed failure of polarized martensitic steels. *Corrosion* (Houston, TX, USA) 1969; 25: 353–358.
- Beck W, Bockris JO'M, Genshaw MA, Subramanian PK. Diffusivity and solubility of hydrogen as a function of composition in Fe-Ni alloys. *Metall Trans* 1971; 2: 883–888.
- Berkowitz BJ, Heubaum FH. The role of hydrogen in sulfide stress cracking of low alloy steels. *Corrosion* (Houston, TX, USA) 1984; 40: 240–245.
- Berkowitz B, Horowitz H. The role of H_2S in the corrosion and hydrogen embrittlement of steel. *J Electrochem Soc* 1982; 129: 468–474.
- Bernstein IM, Thompson AW. Effect of metallurgical variables on environmental fracture of steels. *Int Mater Rev* 1976; 21: 269–287.
- Bhole SD, Nemade JB, Collins L, Cheng L. Effect of nickel and molybdenum additions on weld metal toughness in a submerged arc welded HSLA line-pipe steel. *J Mater Process Tech* 2006; 173: 92–100.
- Biagiotti S. Effect of Ni content and tempering temperature on SSC resistance in modified 4340 steels. In: *Corrosion 95*. Paper No. 64. Houston, TX, USA: NACE International, 1995.

- Borik F, Anselme OR, deSivry B, Boussel P, Bonnet C. SSC resistance of electron beam welded, Q&T X60, X80 and X100 line pipe steels. In: Corrosion 82. Paper No. 139. Houston, TX, USA: NACE International, 1982.
- Boyer HE, editor. ASM metals handbook, vol. 11, 8th ed. Metals Park, OH: ASM International, 1976.
- Bryhan A. The effect of testing procedure on implant test results. *Weld J* 1981; 59: 169–176.
- Bush D, Brown J, Lewis K. An overview of NACE international standard MR0103 and comparison with MR0175. In: Corrosion, 2004. Paper No. 04649. New Orleans, LA: NACE International, 2004.
- Campbell FC. Elements of metallurgy and engineering alloys. Metals Park, OH: ASM International, 2008.
- Carneiro R, Ratnapuli R, Freitas Cunha Lins V. The influence of chemical composition and microstructure of API linepipe steels on hydrogen induced cracking and sulfide stress corrosion cracking. *Mater Sci Eng A* 2003; A357: 104–110.
- Chavane A, Habashi M, Pressouyre GM, Galland J. High-strength steels with improved sulfide stress cracking resistance. *Corrosion* (Houston, TX, USA) 1986; 42: 54–61.
- Cheng KC, Ou J-W. Joule-Thomson effects on turbulent graetz problem for gas flows in pipes with uniform wall temperature. *Can J Chem Eng* 1978; 56: 31–36.
- Colwell JA, Payer JH, Boyd WK. Performance of steels in high pressure environments containing low H₂S concentrations. In: Corrosion 86. Paper No. 168. Houston, TX, USA: NACE International, 1986.
- Craig B. The effect of nickel on hydrogen cracking resistance in low alloy steels – a review. *Corrosion* (Houston, TX, USA) 1982; 38: 457–463.
- Craig BD. Review of nickel's role in sulfide stress cracking of low alloy steels. *Corrosion* (Houston, TX, USA) 1988; 44: 776–782.
- Craig B, Krauss G. The structure of tempered martensite and its susceptibility to hydrogen stress cracking. *Metall Trans A* 1980; 11A: 1799–1808.
- Craig B, Brownlee J, Bruno T. The role of nickel in the sulfide stress cracking of low-alloy steels. *Corrosion* (Houston, TX, USA) 1990; 46: 142–146.
- Craig B, Brownlee J, Bruno T. Sulfide stress cracking of nickel steels. *Corrosion* (Houston, TX, USA) 1992; 48: 90–97.
- Davis JR. Fracture mechanics properties of carbon and alloy steels, vol. 19. ASM metals handbook. Metals Park, OH: ASM International, 1990.
- Davis JR, editor. Alloying: understanding the basics. Metals Park, OH: ASM International, 2001.
- DeRetana A, Doane D. Predicting hardenability of carburizing steels. *Met Prog* 1971: 65–69.
- Devanathan MAV, Stachurski Z. The adsorption and diffusion of electrolytic hydrogen in palladium. *Proc R Soc Lond A* 1962; 270: 90–102.
- Dieter GE. Mechanical metallurgy SI metric. London, UK: McGraw-Hill, 1986.
- DNV. Cathodic protection design. DNV-RP-B401 recommended practice. Høvik, Norway: DNV, 2010.
- DNV. DNV-OS-F101 offshore standard, submarine pipeline systems. Høvik, Norway: DNV, 2012.
- Dunlop A. Stress corrosion cracking of low strength, low alloy nickel steels in sulfide environments. *Corrosion* (Houston, TX, USA) 1978; 34: 88–96.
- Dvoracek L. Sulfide stress corrosion cracking of steel. *Corrosion* (Houston, TX, USA) 1970; 26: 177–188.
- EFC. European Federation of Corrosion Publications NUMBER 16, a working party report on guidelines on materials requirements for carbon and low alloy steels for H₂S-containing environments in oil and gas production, 3rd ed. Leeds, UK: Maney Publishing, 2009.
- Erlings JG, De Groot HW, Nauta J. The effect of slow plastic and elastic straining on sulphide stress cracking and hydrogen embrittlement of 3.5 wt% Ni steel and API 5L X60 pipeline steel. *Corros Sci* 1987; 27: 1153–1167.
- Eroğlu M. Effect of nickel with chromium on microstructure and toughness of heat affected zone in low carbon steel. *Sci Technol Weld Joining* 2002; 7: 217–223.
- Eroglu M, Aksoy M. Effect of nickel on microstructure and mechanical properties of heat affected zone of low carbon steel. *Mater Sci Technol* 2002; 18: 35–40.
- Farrar RA. 1.5%–3.5% nickel cryogenic steels. In: The alloy tree – a guide to low alloy steels, stainless steels, and nickel-base alloys. Cambridge, UK: CRC Press-Woodhead Publishing, 2004: 28–29.
- Fraser J, Eldredge G, Treseder R. Laboratory and field methods for quantitative study of sulfide corrosion cracking. *Corrosion* (Houston, TX, USA) 1958; 14: 37–43.
- Gangloff RP. Hydrogen assisted cracking of high strength alloys. In: Milne I, Ritchie RO, Karihaloo B, editors. Comprehensive structural integrity, vol. 6. New York: Elsevier, 2003: 31–101.
- Garber R. Higher hardenability low alloy steels for H₂S-resistant oil country tubulars. *Corrosion* (Houston, TX, USA) 1983; 39: 83–91.
- Garber R, Wada T, Fletcher EB, Cox TB. Sulfide stress cracking resistant steels for heavy section wellhead components. *J Mater Eng* 1985; 7: 91–103.
- Gerberich WW, Chen YT. Hydrogen-controlled cracking – an approach to threshold stress intensity. *Metall Trans A* 1975; 6: 271–278.
- Glasstone S. An introduction to electrochemistry. New Delhi: Affiliated East-West Press, 1942.
- Gooch TG. SCC of ferritic steel weld metal – the effect of nickel. Part 2 – results and discussion. *Met Constr* 1982a; 14: 73–79.
- Gooch TG. SCC of ferritic steel weld metal – the effect of nickel. Part 1 – introduction and experimental. *Met Constr* 1982b; 14: 29–33.
- Gordine J. The weldability of some Arctic-grade line-pipe steels. *Weld J* 1977; 56: 201–210.
- Grange R. Estimating the hardenability of carbon steels. *Metall Trans* 1973; 4: 2231–2244.
- Grobner P, Sponseller D, Diesburg D. The effects of processing variables on mechanical properties and sulfide stress cracking resistance of SAE 4135 steel modified with 0.75 percent, Mo and 0.035 percent Cb. *J Manuf Sci Eng* 1976; 98: 708–716.
- Grong O, Matlock DK. Microstructural development in mild and low-alloy steel weld metals. *Int Mater Rev* 1986; 31: 27–48.
- Hamby TW. Deep, high-pressure sour gas wells – an industry challenge. In: Annual Meeting Papers, Division of Production. Paper No. API-75-C001. Dallas, TX, USA: American Petroleum Institute, 1975.
- Heidersbach R. Materials. In: Metallurgy and corrosion control in oil and gas production. Wiley series in corrosion. Hoboken, NJ: John Wiley & Sons, 2010: 36–74.

- Hirth JP. Effects of hydrogen on the properties of iron and steel. *Metall Trans A* 1980; 11A: 861–890.
- Hope I. World perspectives for the oil and gas industry. In: *Rio Oil and Gas*. Rio de Janeiro, Brazil: Instituto Brasileiro de Petróleo, Gás, e Biocombustíveis, 2008.
- Horn AM. Materials Challenges in the Arctic. In: *Robuste materialvalg i oljeindustrien*. Stavanger, Norway: Norsk Forening for Vedlikehold, 2012.
- Horn AM, Hauge M. Material challenges for arctic offshore applications, a reliability study of fracture of a welded steel plate based on material toughness data at -60°C. In: *Proceedings of the Twenty-First International Offshore and Polar Engineering Conference*. Maui, Hawaii: The International Society of Offshore and Polar Engineers, 2011: 393–401.
- Horn A, Østby E, Hauge M, Aubert J-M. Robust material qualification for Arctic applications. In: *Proceedings of the Twenty-Second International Offshore and Polar Engineering Conference*. Rhodes, Greece: International Society of Offshore and Polar Engineers, 2012: 290–296.
- Huang Y, Nakajima A, Nishikata A, Tsuru T. Effect of mechanical deformation on permeation of hydrogen in iron. *ISIJ Int* 2003; 43: 548–554.
- Hudgins C, McGlasson RL, Mehdizadeh P, Rosborough WM. Hydrogen sulfide cracking of carbon and alloy steels. *Corrosion* (Houston, TX, USA) 1966; 22: 238–251.
- Ikeda A, Kaneko T, Ando Y. On the evaluation method of sulfide stress cracking susceptibility of carbon and low alloy steels. *Corros Sci* 1987; 27: 1099–1115.
- ISO. Petroleum and natural gas industries – induction bends, fittings and flanges for pipeline transportation systems. ISO 15590-1:2009 standard. Geneva, Switzerland: ISO, 2009.
- ISO. Petroleum and natural gas industries – Arctic offshore structures. ISO 19906. Geneva, Switzerland: ISO, 2010a.
- ISO. Petroleum, petrochemical and natural gas industries – materials selection and corrosion control for oil and gas production systems. ISO 21457:2010 standard. Geneva, Switzerland: ISO, 2010b.
- Jarvis A, Bulloch J. The effect of nickel content on the environmental assisted cracking (EAC) behaviour of low alloy steels in sour environments – a review. *Int J Pres Ves Pip*, 1992; 49: 271–307.
- Jatczak CF. Hardenability curves. In: B. Bardes, editor. *Properties and selection: irons and steels*, vol. 1. ASM handbook. Metals Park, OH: ASM, 1978: 497–525.
- Jolley W. Effect of Mn and Ni on impact properties of Fe and Fe-C alloys. *JISI* 1968a; 206: 170–173.
- Jolley W. Influence of a 3.28 pct Nickel addition on the yield and fracture behavior of alpha iron. *Trans Metall AIME* 1968b; 242: 306–314.
- Kaneko T, Ikeda A. Influence of small amounts of nickel addition on sulfide stress cracking susceptibility in low-alloy steel. *Trans ISIJ* 1988; 28: 575–577.
- Kappes M, Frankel GS, Thodla R, Mueller M, Sridhar M, Carranza RM. Hydrogen permeation and corrosion fatigue crack growth rates of X65 pipeline steel exposed to acid brines containing thiosulfate or hydrogen sulfide. *Corrosion* (Houston, TX, USA) 2012; 68: 1015–1028.
- Kawashima A, Hashimoto K, Shimodaira S. Hydrogen electrode reaction and hydrogen embrittlement of mild steel in hydrogen sulfide solutions. *Corrosion* (Houston, TX, USA) 1976; 32: 321–331.
- Kharionovskii VV. Strength in operation of gas pipelines in the Far North. *Strength Mater* 1983; 15: 1633–1639.
- Kim Y, Kim HJ, Morris JW. The influence of precipitated austenite on hydrogen embrittlement in 5.5Ni steel. *Metall Trans A* 1986; 17: 1157–1164.
- Kimura M, Totsuka N, Kurisu T, Amano K, Matsuyama J, Nakai Y. Sulfide stress corrosion cracking of line pipe. *Corrosion* (Houston, TX, USA) 1989; 45: 340–346.
- Kirkaldy J, Feldman S. Optimization of steel hardenability control. *J Heat Treat* 1989; 7: 57–64.
- Koistinen DP, Marburger RE. A general equation prescribing the extent of the austenite-martensite transformation in pure iron-carbon alloys and plain carbon steels. *Acta Metall* 1959; 7: 59–60.
- Krauss G. Steels: heat treatment and processing principles, Metals Park, OH: ASM International, 1989.
- Krauss G. Hardness and hardenability. In: *Steels: processing, structure, and performance*. Chapter 16. Metals Park, OH: ASM International, 2005a: 297–326.
- Krauss G. Bainite. In: *Steels: processing, structure, and performance*. Chapter 6. Metals Park, OH: ASM International, 2005b: 87–100.
- Krog K, Qvale AH. Low alloy steels for large bore subsea connectors. In: *Robuste materialvalg i oljeindustrien*. Stavanger, Norway: Norsk Forening for Vedlikehold, 2012.
- Kuch ER. Hardenability of carbon and low-alloy steels. In: *Properties and selection: irons, steels, and high-performance alloys*, vol. 1. ASM handbook. Metals Park, OH: ASM International, 1990: 451–463.
- Lancaster J. Handbook of structural welding: processes, materials and methods used in the welding of major structures, pipelines and process plant. Cambridge, England: Abington Publishing, 1997.
- Latanision RM, Gastine OH, Compeau CR. Stress corrosion cracking and hydrogen embrittlement: differences and similarities. In: Forouli Z, editor. *Environment-sensitive fracture of engineering materials*. Chicago, IL: Metallurgical Society of AIME, 1977: 48–70.
- Leslie WC, Sober RJ, Babcock SG. Plastic flow in binary substitutional alloys of BCC iron – effects of strain rate, temperature and alloy content. *Trans ASM* 1969; 62: 690–710.
- Lessar J, Gerberich W. Grain size effects in hydrogen-assisted cracking. *Metall Trans A* 1976; 7: 953–960.
- Malakondaiah G, Srinivas M, Rama Rao P. Ultrahigh-strength low alloy steels with enhanced fracture toughness. *Prog Mater Sci* 1997; 42: 209–242.
- Mc Nabb A, Foster PK. A new analysis of the diffusion of hydrogen in iron and ferritic steels. *Trans Metall AIME* 1963; 227: 618–627.
- McMahon C, Cianelli A, Feng H. The influence of Mo on P-induced temper embrittlement in Ni-Cr steel. *Metall Trans A* 1977; 8: 1055–1057.
- Motoda K, Yamane Y. Stress corrosion cracking of steels in aqueous solution of low hydrogen sulfide concentration. In: 101st ISIJ meeting. Lecture No. S477, 1981.
- Motoda K, Yamane Y, Uesugi Y, Nakai Y. Effect of potential on sulfide stress corrosion cracking of steels. In: 101st ISIJ meeting. Lecture No. S478, 1981.
- Mukerjee D, Mediratta SR, Ramaswamy V. Dilatometric study on some medium carbon constructional steels. *Trans ISIJ* 1986; 27: 108–114.

- Mulford RA, McMahon CJ Jr, Pope DP, Feng HC. Temper embrittlement of Ni-Cr steel by antimony: III. Effects of Ni and Cr. *Metall Trans A* 1976a; 7A: 1269–1274.
- Mulford RA, McMahon CJ Jr, Pope DP, Feng HC. Temper embrittlement of Ni-Cr steels by phosphorus. *Metall Trans A* 1976b; 7: 1183–1195.
- NACE. Laboratory testing of metals for resistance to sulfide stress cracking and stress corrosion cracking in H₂S environments. NACE TM 0177-96 standard test method. Houston, TX, USA: NACE International, 1996.
- NACE. Four-point bend testing (v2). NACE TG085 (draft specification). Houston, TX, USA: NACE International, 2014.
- NACE-ISO. Petroleum and natural gas industries – materials for use in H₂S-containing environments in oil and gas production. NACE MR0175/ISO 15156-2 standard. Houston, TX, USA: NACE International/ISO, 2001.
- Narasimha Rao BV, Thomas G. Structure-property relations and the design of Fe-4Cr-C base structural steels for high strength and toughness. *Metall Trans A*, 1980; 11A: 441–457.
- NORSOK. Material data sheets and element data sheets for piping. NORSOK standard M-630. Straume, Norway: Norwegian Piping, 2010: 1–133.
- Okada H, Yukawa K, Tamura H. Transition of cracking mechanisms from active path corrosion to hydrogen embrittlement in high strength steels in a boiling nitrate solution. *Corrosion* (Houston, TX, USA) 1976; 32: 201–203.
- Oriani R. The diffusion and trapping of hydrogen in steel. *Acta Metall* 1970; 18: 147–157.
- Oriani R. Hydrogen – the versatile embrittler. *Corrosion* (Houston, TX, USA) 1987; 43: 390–397.
- Pargeter RJ. The effect of low H₂S concentrations on welded steels. In: *Corrosion 2000*. Paper No. 00143. Houston, TX, USA: NACE International, 2000.
- Paterson P. Material challenges in upstream oil and gas in the future. In: *Robuste materialvalg i oljeindustrien*. Stavanger, Norway: Norsk Forening for Vedlikehold, 2012.
- Payer JH, Pednekar SP, Boyd WK. Sulfide Stress Cracking Susceptibility of Nickel Containing Steels. *Metall Trans A* 1986; 17: 1601–1610.
- Petch NJ. The influence of some substitutional alloys on the cleavage of ferritic steels. *Acta Metall* 1987; 35: 2027–2034.
- Philip TV, McCaffrey TJ. Ultrahigh-strength steels. In: *Properties and selection: irons, steels, and high-performance alloys*, vol. 1. ASM handbook. Metals Park, OH: ASM International, 1990.
- Prabhudev KH. Handbook of heat treatment of steels. Noida, UT, India: Tata McGraw-Hill, 1988.
- Pressouyre G. A classification of hydrogen traps in steel. *Metall Mater Trans A* 1979; 10A: 1571–1573.
- Pressouyre G. Trap theory of hydrogen embrittlement. *Acta Metall* 1980; 28: 895–911.
- Pressouyre G, Bernstein I. A quantitative analysis of hydrogen trapping. *Metall Trans A* 1978; 9: 1571–1580.
- Roe G, Bramfitt BL. Notch toughness of steels. In: *Properties and selection: irons, steels, and high-performance alloys*, vol. ASM handbook. Metals Park, OH: ASM International, 1990: 737–754.
- Saenz de Santa Maria M, Turnbull A. The effect of H₂S concentration and pH on the cracking resistance of AISI 410 stainless steel in 5% brine. *Corros Sci* 1989; 29: 69–88.
- Sarikaya M, Jhingan AK, Thomas G. Retained austenite and tempered martensite embrittlement in medium carbon steels. *Metall Trans A* 1983; 14A: 1121–1133.
- Sarno D, Bruner J, Kampschaefer G. Fracture toughness of 5% nickel steel weldments. *Weld J* 1974; 53: 486–494.
- Schillmoller CM, Craig BD. Nickel steels in arctic service. In: *Corrosion 87*. Paper No. 473. San Francisco, CA: NACE, 1987.
- Schmid G. The resistance of nickel containing steels and weld metals to sulfide stress corrosion cracking. *Mater Perform* 1980; 19: 9–18.
- Scoonover T, Arnsen H. Hardenability of low- and medium-carbon Mn-Cr-Ni-Mo steels. *J Heat Treat* 1984; 3: 183–192.
- Shaughnessy JM, Romo LA, Soza RL. Problems of ultra-deep high-temperature, high-pressure drilling. In: *SPE Annual Technical Conference and Exhibition*. Paper No. SPE-84555-MS. Denver, CO: Society of Petroleum Engineers, 2003.
- Shoosmith DW, Taylor P, Bailey MG, Owen DG. The formation of ferrous monosulfide polymorphs during the corrosion of iron by aqueous hydrogen sulfide at 21°C. *J Electrochem Soc* 1980; 127: 1007–1015.
- Siebert C, Doane D, Breen D. The hardenability of steels: concepts, metallurgical influences, and industrial applications. Metals Park, OH: ASM International, 1977.
- Smith JS, Miller JDA. Nature of sulphides and their corrosive effect on ferrous metals: a review. *Br Corros J* 1975; 10: 136–143.
- Snape E. Sulfide stress corrosion of some medium and low alloy steels. *Corrosion* (Houston, TX, USA) 1967; 23: 154–172.
- Snape E. Discussion of “Factors in sulfide stress cracking of high strength steels.” *Corrosion* (Houston, TX, USA) 1968a; 24: 36–37.
- Snape E. Roles of composition and microstructure in sulfide cracking of steel. *Corrosion* (Houston, TX, USA) 1968b; 24: 261–282.
- Snape E, Schaller F, Forbes Jones R. A method for improving hydrogen sulfide accelerated cracking resistance of low alloy steels. *Corrosion* (Houston, TX, USA) 1969; 25: 380–388.
- Solana F, Takamada C, Bernstein IM, Thompson W. The role of retained austenite in stress corrosion cracking of steels. *Metall Trans A* 1987; 18A: 1023–1028.
- Sponseller D, Garber R, Straatmann JA. Effect of microstructure on sulfide-stress-cracking resistance of high-strength casing steels. In: *Abrams H, Clark E, Hood J, Seth B, editors. Micon 82: optimization of processing, properties, and service performance through microstructural control*, ASTM SRP 792. West Conshohocken, PA: ASTM International, 1982: 172–204.
- Total. General specification piping valves vessels. GS EP PVV 142. Île-de-France, France: Total, 2005a: 1–65.
- Total. General specification pipelines – risers, fabrication of seamless pipes for pipelines (intermediate and severe sour service). Total Exploration & Production GS EP PLR 211. Île-de-France, France: Total, 2005b.
- Treseder R, Swanson T. Factors in sulfide stress cracking of high strength steels. *Corrosion* (Houston, TX, USA) 1968; 24: 31–37.
- Tsai SY, Shih HC. Correlation between acoustic emission signals and hydrogen permeation in high strength, low alloy steel cracking in wet H₂S. *J Electrochem Soc* 1998; 145: 1968–1976.
- Turn JC, Wilde BE, Troianos CA. On the sulfide stress cracking of line pipe steels. *Corrosion* (Houston, TX, USA) 1983; 39: 364–370.
- Turnbull A, Carroll M. The effect of temperature and H₂S concentration on hydrogen diffusion and trapping in a 13% Cr martensitic stainless steel in acidified NaCl. *Corros Sci* 1990; 30: 667–679.

- Turnbull A, Carroll M, Ferriss D. Analysis of hydrogen diffusion and trapping in a 13% chromium martensitic stainless steel. *Acta Metall* 1989; 37: 2039–2046.
- Turnbull A, Saenz de Santa Maria M, Thomas N. The effect of H₂S concentration and pH on hydrogen permeation in AISI 410 stainless steel in 5% NaCl. *Corros Sci* 1989; 29: 89–104.
- Uhlig HH. Discussion of “Stress corrosion cracking of low strength, low alloy nickel steels in sulfide environments”. *Corrosion* (Houston, TX, USA) 1978; 34: 364–365.
- VGS. AISI 4340 or BS 970 grade 817M40 low alloy steel forgings based on API, ISO, and other industry standards (NON-NACE). VGS 5.111.1. VGS, 2012a.
- VGS. High strength 4330 modified low alloy steel forgings for use in high capacity running tools, includes mandatory approved vendor list. VGS 5.111.3. VGS, 2012b.
- VGS. 1Ni1/4Mo-UNS K11260 (modified) bainitic high strength low alloy steel for GE Oil and Gas pup & transition piece forgings for low temperature service, with mandatory approved vendor list. VGS 5.113.4. VGS, 2012c.
- VGS. 33NiCrMoV14-5 (modified) low alloy steel forgings for GE Oil and Gas clamp connector. VGS 5-113-3. VGS, 2012d: 1–10.
- VGS. 1Ni1/4Mo-UNS K11260 (modified) bainitic high strength low alloy steel for GE Oil and Gas hub and cap forgings for low temperature service, with mandatory approved vendor list. VGS 5.113.1. VGS, 2013a.
- VGS. 1Ni1/4Mo bainitic high strength low alloy steel forgings. VGS 5.113.2. VGS, 2013b.
- Viswanathan R. Temper embrittlement in a Ni-Cr steel containing phosphorus as impurity. *Metall Trans* 1971; 2: 809–815.
- Vander Voort GF. Atlas of time-temperature diagrams for iron and steels. Metals Park, OH: ASM International, 1991.
- Wang W, Liu S. Alloying and microstructural management in developing SMAW electrodes for HSLA-100 steel. *Weld J* 2002; 81: 132–145.
- Webster SE, Austen IM, Rudd WJ. Technical steel research, properties and service performance, fatigue, corrosion fatigue and stress corrosion of steels for offshore structures. Report published by the Commission of the European Communities, 1985.
- Welsch MT, Bruch D, Østby E. Forgings for low temperature applications – influences of the alloying concept and advanced forging procedures on impact strength and fracture toughness. In: *Proceedings of the Twenty-First International Offshore and Polar Engineering Conference*. Maui, Hawaii: International Society of Offshore and Polar Engineers, 2011: 377–383.
- Wilde B. Mechanism of cracking of high strength martensitic stainless steels in sodium chloride solutions. *Corrosion* (Houston, TX, USA) 1971; 27: 326–333.
- Wilde B, Doyle M. A comparison between threshold stress and “crack initiation” stress intensity for sulfide stress corrosion cracking. *Corrosion* (Houston, TX, USA) 1979; 35: 273–276.
- Wilde BE, Kim CD, Turn JC. The influence of noble metal additions on the sulfide corrosion performance of AISI 4130 steel. *Corrosion* (Houston, TX, USA) 1982; 38: 515–524.
- Williamson DL, Schupmann RG, Materkowski JP, Krauss G. Determination of small amounts of austenite and carbide in hardened medium carbon steels by Mössbauer spectroscopy. *Metall Trans A* 1979; 10A: 379–382.
- Yamane Y, Totsuka N, Kimura M, Kurisu T, Motoda K, Nakai Y. Effect of Ni on sulfide stress corrosion cracking in low alloy steels. In: *Corrosion 86*. Paper No. 167. Houston, TX, USA: NACE International, 1986.
- Yoshino Y. Low alloy steels in hydrogen sulfide environment. *Corrosion* (Houston, TX, USA) 1982; 38: 156–167.
- Yoshino Y. Metallurgical influences on the hydrogen uptake by steel in H₂S environment. *Corrosion* (Houston, TX, USA) 1983; 39: 435–443.
- Yoshino Y, Minozaki Y. Sulfide stress cracking resistance of low-alloy nickel steels. *Corrosion* (Houston, TX, USA) 1986; 42: 222–233.
- Yurioka N, Suzuki H, Ohshita S, Saito S. Determination of necessary preheating temperature in steel welding. *Weld J* 1983; 62: 147–153.
- Zakroczymski T. Activation of the iron surface to hydrogen absorption resulting from a long cathodic treatment in NaOH solution. *J Electrochem Soc* 1985a; 132: 2548–2552.
- Zakroczymski T. The effect of straining on the transport of hydrogen in iron, nickel, and stainless steel. *Corrosion* (Houston, TX, USA) 1985b; 41: 485–489.
- Zhang Z, Farrar R. Influence of Mn and Ni on the microstructure and toughness of C-Mn-Ni weld metals. *Weld J* 1997; 76: 183–196.
- Zhirafar S, Rezaeian A, Pugh M. Effect of cryogenic treatment on the mechanical properties of 4340 steel. *J Mater Process Tech* 2007; 186: 298–303.



Mariano Kappes obtained his diploma in materials engineering in 2006 at the Instituto de Tecnología Prof. J. Sabato in Argentina. He joined the Fontana Corrosion Center at the Ohio State University in 2007, where he obtained his PhD in materials science and engineering in 2011 under Prof. Gerald Frankel's guidance. His PhD thesis, focused on corrosion fatigue of carbon steels in thiosulfate solutions, was recognized with the Morris Cohen Graduate Student award (Electrochemical Society). From 2012 to 2013, he held a postdoctoral research position at the Corrosion and Reliability

Engineering Center at the University of Akron. In 2014, he joined the Argentine Commission of Atomic Energy, where he is currently researching on stress corrosion cracking and hydrogen embrittlement of steels and magnesium alloys and localized corrosion of stainless steels and nickel alloys.



Mariano Iannuzzi graduated from The Ohio State University (Fontana Corrosion Center), receiving the Morris Cohen Award (Electrochemical Society) and the NACE Foundation Book Award and NACE International Marcel Pourbaix award for his work on corrosion

inhibition of aluminum alloys by vanadates. Dr. Iannuzzi is currently a principal corrosion engineer at General Electric, Norway. Dr. Iannuzzi is responsible for the development, management, and execution of research and development activities on materials and corrosion science topics of interest to GE Oil and Gas subsea systems. Before GE, Dr. Iannuzzi worked as an assistant professor in the Chemical and Biomolecular Engineering Department at the University of Akron.



Raúl B. Rebak studied chemical engineering at the University of Misiones (Argentina) between 1974 and 1982. He then received a national scholarship to work at the Argentine Commission of Atomic Energy between 1983 and 1988. In 1989, he joined the Ohio State University Materials Science Department, where he received a PhD degree in corrosion and metallurgy in 1993. From 1996 to 2000, Raul worked as a corrosion engineer at Haynes International in Indiana, and from 2001 to 2007, at the University of California Lawrence Livermore National Laboratory. In 2007, Raul joined General Electric Global Research Center in Schenectady, NY, where he provides his experience in corrosion science and corrosion engineering applications in areas such as nuclear, oil and gas, energy storage, aviation, etc. Raúl has more than 30 years' experience and published over 200 technical articles in corrosion. He is very active in technical societies and technical committees at, for example, ASTM International, NACE International, ASM International, TMS,

where he served as chair of numerous committees and symposia. He was chair of NACE International San Francisco Bay section and of ASM International Eastern New York chapter. Raúl is a fellow of NACE International, The Corrosion Society.



Ricardo M. Carranza studied physical chemistry at the University of Córdoba (Argentina) between 1975 and 1979. In 1980, he received a national scholarship to work on his PhD thesis at the Argentine Commission of Atomic Energy. In 1986, he received a PhD degree in chemistry at the University of Buenos Aires. Since 1986, Ricardo has been working as a corrosion scientist at the Argentine Commission of Atomic Energy doing research in the nuclear area, stress corrosion cracking, localized corrosion, and hydrogen permeation of highly corrosion resistant alloys. He teaches corrosion courses at the Instituto Sabato since 1994, becoming the managing director of the master's degree program in materials science in 2008. Ricardo has more than 30 years' experience and published over 100 technical articles in corrosion. He is member of several technical societies in Argentina (SAM and AATN). He is member of NACE, where he participates in the International Research Committee and as chair of the Corrosion in Nuclear Systems Symposium NACE 2009 International Conference. He was the chair of the organizing committee of the symposium "Scientific Basis for Nuclear Waste Management XXXV", MRS Meeting, 2011, Buenos Aires, Argentina.